Getting Ahead of the Curve: Assessment of New Photovoltaic Module Reliability Risks Associated With Projected Technological Changes

Jarett Zuboy ⓘD, Martin Springer ⓘD, Elizabeth C. Palmiotti ⓘD, Joseph Karas ⓘD, Brittany L. Smith ⓘD, Michael Woodhouse ⓘD, and Teresa M. Barnes ⓘD

Abstract*—Maintaining the reliability of photovoltaic (PV) modules in the face of rapidly changing technology is critical to maximizing solar energy's contribution to global decarbonization. Our review describes expected changes in PV technology and their impacts on performance and reliability. We leverage PV market reports, interviews with PV researchers and other industry stakeholders, and peer-reviewed literature to narrow the multitude of possible changes into a manageable set of 11 impactful trends likely to be incorporated in near-term crystalline-silicon module designs. We group the trends into four categories (module architecture, interconnect technologies, bifacial modules, and cell technology) and explore the drivers behind the changes, their interactions, and associated reliability risks and benefits. Our analysis identifies specific areas that would benefit from accelerating the PV reliability learning cycle to assess emerging module products and designs more accurately. We recommend that researchers continue tracking module technologies and their reliability implications, so efforts can be focused on the most impactful trends. As the rapid technological turnover continues, it is also critical to incorporate fundamental knowledge into models that can predict module reliability. Predictive capabilities complete the PV reliability learning cycle—reducing the time required to assess new designs and mitigating the risks associated with large-scale deployment of new products.

***Index Terms*—Bifacial, cell, degradation, durability, forecast, interconnection, module, photovoltaic (PV), projection, reliability, solar, technology, trend.**

I. INTRODUCTION

SOLAR photovoltaic (PV) technology is central to global decarbonization efforts, requiring deployments of at least 630 GW/year by 2030 [1]. Reliable PV modules and systems are key to meeting these ambitious deployment targets [2]. Reliable modules last longer, produce more energy, are more cost-competitive, and have less environmental impact [2], [3]. They can also help maintain energy resilience during catastrophic events. Moreover, reliability builds confidence in PV technology among potential end users and financiers, enabling faster and more widespread deployment. PV has been reliable to date, with product warranties spanning decades and less than 1% of modules installed in the United States failing within their first five years [4]. Degradation rates have remained mostly constant between less expensive modern modules and previous generations of technologies. However, multiple factors will affect future module reliability and efforts to extend module lifetimes past 30 years [5].

First, an exponential deployment growth curve along with rapidly evolving technology means a large proportion of technologies in PV systems at any given time will be new. Such technologies may not have a field history, they may be deployed in environments where they have not been deployed before, or both. Most will lack the three years of data required to calculate accurate degradation rates. The rapid pace of introducing new PV technologies into the field creates a potentially greater risk of encountering premature failures and long-term reliability issues [6].

Second, manufacturers are under pressure to reduce module prices while increasing efficiency, resulting in PV technology changes [4]. Technology choices can also be influenced by changes in the global PV supply chain [7]. These technology changes often lead to higher performance, lower cost, or both, but some may increase reliability risks. One well-known example is the failure of backsheets made of a type of AAA polyamide, which entered the market in 2010. The AAA backsheets became popular because of their low cost and because the supply of conventional backsheets was constrained. These AAA backsheets passed standard damp-heat and ultraviolet (UV) light tests, but many began cracking after five to ten years owing to mechanical stresses from production and environmental exposure that had not been part of standard testing [4]. In addition to the impacts of individual changes, the complex interactions among multiple module materials exacerbate the reliability impacts of technological change [8].

Finally, there is pressure to increase module lifetimes. Typical module warranties were 10 years in 1990 and 30 years in 2020 [6], with one product achieving a 40-year warranty in 2022 [9]. The U.S. Department of Energy is targeting a 50-year useful module life [10]. These expectations call for module design choices, manufacturing processes, and testing that can enable longer lifetimes, while longer lifetimes create additional uncertainty around very long-term degradation and failure rates. Current standards and new accelerated tests have effectively reduced premature failures [11], but the PV community knows less about degradation after 10 or 20 years because systems using current technology have not yet been deployed in the field that long.

To ensure that PV can continue driving global decarbonization under these circumstances, the PV community must get ahead of the curve on module reliability. In their review of module degradation and failure phenomena, Aghaei et al. [8] call for research on new materials and module designs as they are introduced, considering reliability along with performance, cost, and sustainability. They also stress the importance of developing tests that can predict long-term reliability in the context of multiple materials and multiple stresses that vary over time [12]. Reliability researchers have started to make progress on this effort but it is difficult to keep up with product development and deployment cycles [6], [13].

We contribute toward this effort by identifying and linking specific new module technology trends with potential reliability impacts. The PV module industry uses different trade names and descriptions for many of these technology changes, which we define, describe, and categorize for clarity. For each of the 11 trends, we analyze technology drivers (e.g., improved performance, cost, or sustainability), deployment projections, reliability implications, options for mitigating reliability risks, and the need for additional research and testing. We also explore reliability-related interactions among multiple trends. The results are meant to provide an early step toward identifying future reliability issues that have yet to materialize owing to the lack of historical field data for novel technologies. We conclude by suggesting areas related to the reliability of new module trends that would benefit from additional research as well as the development of standards and testing.

Note that we address only crystalline-silicon PV technology and exclude other module technologies including those based on thin films and tandem cells. Crystalline-silicon technology accounts for more than 80% of PV installed in the United States, accounts for more than 90% worldwide, and is projected to remain dominant over the next decade [14], [15]. Thin-film modules are primarily made by a single manufacturer and do not have as much variation in technology changes or descriptions of those changes. They will be covered in future work.

II. ASSESSING MODULE TECHNOLOGY TRENDS AND RELIABILITY IMPLICATIONS

We synthesize a range of sources to identify likely and impactful near-term module technology trends and assess the reliability implications of those trends. Combining information from PV market reports, interviews with PV researchers and other industry stakeholders, and peer-reviewed literature helps link academic and business concerns and better capture rapidly evolving knowledge and viewpoints. Key market sources include the International Technology Roadmap for Photovoltaic (ITRPV) [16], [17], [18], [19], [20], [21], [22], PV Tech [15], and InfoLink [23], [24]. The Acknowledgment section specifies individuals and groups who contributed their expertise.

Fig. 1 highlights the major trends in crystalline-silicon module evolution that we identified, starting in 2014 at the left and proceeding beyond 2022 at the right. First, modules are becoming larger. Second, interconnect technologies are changing from cells with several wide busbars connected by wide ribbons to cells with more numerous, thinner busbars, and ribbons. Furthermore, interconnect changes include a transition to cells connected by wires with or without busbars and approaches with little or no gap between cells such as shingling. Third, modules are switching from monofacial designs, which only convert sunlight at the front of the module, to bifacial designs, which also convert light hitting the back of the module. This change is driving evolution in glass, backsheet, and encapsulant choices. Finally, cell technologies are changing from aluminum back surface field (Al-BSF) cells in the recent past to the p-type passivated emitter and rear cell (PERC) that is dominant today, to the emerging n-type tunnel oxide passivating contact (TOPCon) and silicon heterojunction (SHJ) technologies.

The icons at the bottom of Fig. 1 estimate the impact of these trends, showing metrics for typical past, recent, and emerging module technologies that would be used in utility-scale PV systems, based on ITRPV data. In this example, module size increases from 1.7 m^2 in mainstream products sold around 2014 to 2.0 m^2 in recent mainstream products, to 2.5 m^2 and larger in emerging products. Across these same three evolutionary steps, the cell-to-module (CTM) power ratio increases from 99% to 101% and greater. The CTM ratio is calculated by dividing the module power by the total power of the individual cells within the module [25], [26]; a value above 100%—enabled by improved module architectures and interconnection technologies—means an integrated module produces more power than the sum of the individual cells from which it is made. The bifaciality factor is the ratio of a cell's rear efficiency to front efficiency; it improves from zero in the past to almost one in emerging modules. Finally, cell efficiency increases from 18% to 25% and greater. All these trends affect module power. The first icon in each series of icons shows the estimated trend in increased power from 280 peak watts (Wp) to 500 Wp and greater. These power estimates are calculated based on the front side of the modules only. Calculating power contributions from the rear face of bifacial modules is more complex and can depend on PV system design and site characteristics. Bifacial module power ratings are determined following International Electrotechnical Commission (IEC) Standard 60904-1-2, where the measurement and rating are collected on the front but incorporate a previously determined contribution from the rear of the module. For utility-scale applications, a bifacial power gain of around 6.6%–14.5% could be expected [27].
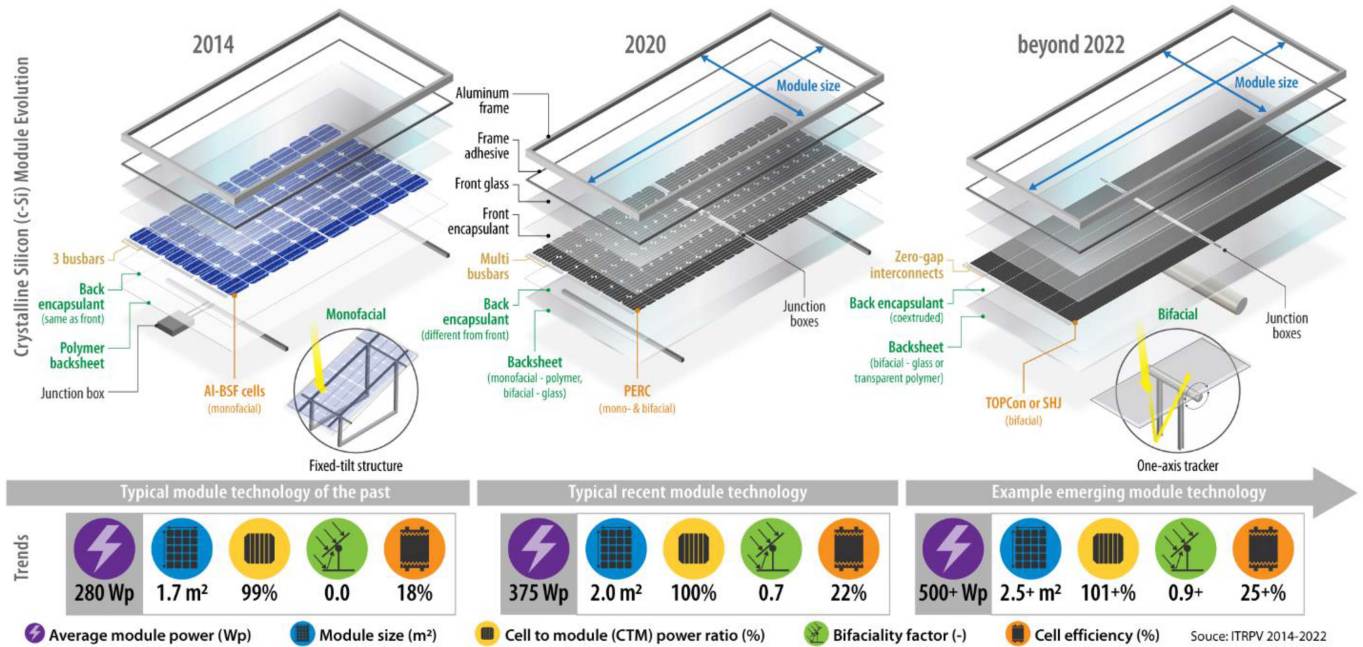
Fig. 1. Overview of crystalline-silicon PV module technology trends, showing the evolution from mainstream, utility-scale module products sold around 2014 to recent mainstream products, to emerging products. The icons at the bottom quantify the approximate impact of these trends across several metrics, based on ITRPV data. The label colors and icons suggest the connections between items in this figure and our technology categories illustrated in Fig. 2.
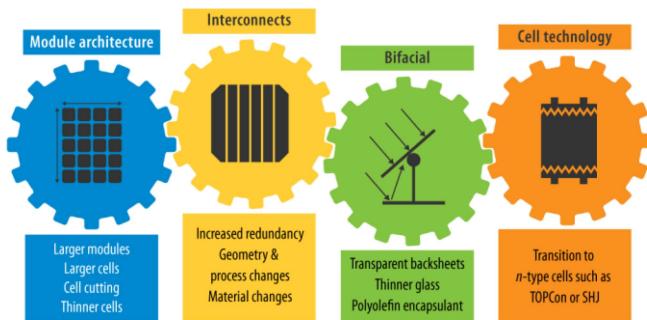

Fig. 2. Total of 11 technology trends analyzed in this article are grouped into four categories. The interlocking-gear motif indicates our analysis of reliability-related interactions among multiple trends.

Ultimately, we chose to analyze the reliability implications of 11 key trends within four categories. The categories and trends are shown in Fig. 2; the figure's interlocking-gear motif suggests the presence of reliability-related interactions among multiple trends. Throughout the article, we illustrate trend trajectories with data from the ITRPV—typically in terms of market shares over time—which enables us to consistently present technology projections through 2032. ITRPV data are collected by surveying PV-related organizations, primarily from Europe [28]. As with all projections, the passage of time exposes deviations between ITRPV projections and real-world technology developments, with deviations typically increasing as projection timespans increase. The accuracy of past projections is analyzed in the ITRPV annual reports and in publications including [28]. We use additional data sources—including PV Tech, InfoLink, academic literature, and expert opinions—to add context to the ITRPV-based projection figures.

We recognize that our limited set of trends does not fully represent the large number of potential variations in commercial module technologies in the context of a rapidly evolving PV industry and the entry of new manufacturers. The proprietary nature of specific module designs and commercial research hinders a shared understanding of product-specific variations, which could have important impacts on reliability even if they are seemingly minor. That said we believe tracking consensus projections of major technology changes, analyzing their reliability implications, and identifying research, testing, and standards-development needs are valuable ways of staying ahead of the curve on module reliability. In the following sections, we analyze the potential reliability implications of each trend individually and as part of integrated systems.

III. MODULE ARCHITECTURE

This section discusses technology trends related to module architecture, including trends toward larger modules, larger cells, cell cutting, and thinner cells. All these interrelated areas have implications for mechanical reliability, such as cell cracking, interconnect breakage or wear out, and associated failure and safety concerns. Cell cracking is an umbrella term for a multistep degradation process that can lead to power loss. We use it as an example of interacting degradation mechanisms to highlight the importance of holistically assessing the reliability implications of interrelated design changes. Cell cracks can be initiated by stresses arising during cell manufacturing as well as during module transportation, installation, and operation. The reliability consequences of cell cracking range from no impact to the formation of hotspots and dead areas leading to module power loss [8]. In one study, 84% of PV modules had at least

one type of crack, but only 60% of the modules had cracks that caused significant power loss [29].

The wide range of reliability consequences stems from the multistep nature of the degradation process. In the first step, cracks are initiated. In the second step, cracks can propagate as the module is subjected to additional stresses over time [8], [30]. In the third step, cell fragments created by cracking can move in response to thermal or mechanical loading, which wears the fragment-bridging metallization and can result in loss of electrical contact and thus power loss [31]. However, the degradation rates for each step depend on a multitude of factors such as module architecture, loading, and the environment. Some cell cracks might never propagate, whereas others might cause power loss immediately. Thus, technology changes can impact all or none of the degradation steps, making the appropriate reliability assessment of multistep degradation processes an ongoing challenge.

For all the module architecture trends, cracking issues can be mitigated through improved manufacturing processes as well as regular sampling and fracture mechanics evaluation of cells from the production line [32]. Cracking-related reliability issues also interact with other trends covered in this article. New interconnect technologies, for example, create redundancy by increasing the number of electrical connections within a cell, which allow cell fragments to remain electrically connected and produce power in the event of cell fracture [33], as discussed in Section IV. Furthermore, glass–glass module architectures—as used for bifacial modules—are heavier than standard glass–backsheet constructions, and manufacturers are trying to reduce weight by using thinner glass sheets, which change the mechanical stresses throughout the package (see Section V).

Cell cracking and mechanical damage are examples of critical areas for further research in determining the relationship between material or design changes and the incidence and timing of long-term module degradation and failure. In addition, the newness of all these trends means more field data must be collected to aid in understanding and predicting potential reliability risks arising during operation. The following sections provide details specific to each module architecture trend, reliability implications, and interactions with other trends.

A. Larger Modules

Increasing the size of PV modules increases the active area of PV systems, and thus, fewer modules are needed to construct a system with a given power output, which tends to reduce installed system costs [34]. In some situations, however, very large modules may require more labor to install than smaller modules [35], [36]; this might increase installation costs if the additional labor cost is not offset by installing fewer modules. Installers must balance these competing considerations.

Nevertheless, the ITRPV projects significant size increases over the next decade. Fig. 3 shows modules smaller than 2.5 m^2 constituting about half of the utility-scale market share in 2021 and then declining to 15% in 2032, at which time 69% are 2.5–3.0 m^2 and 16% are larger than 3.0 m^2. Utility-scale module sizes may stabilize between 2.6 and 3.1 m^2 after the China Photovoltaic Industry Association achieved an
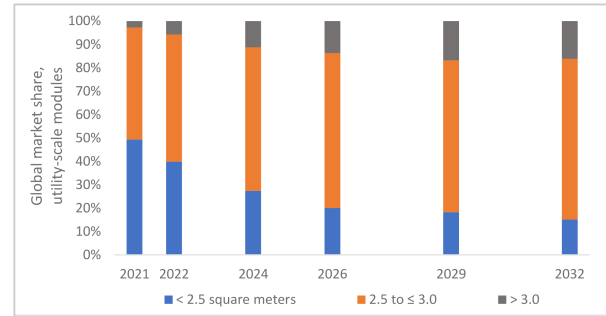

Fig. 3. Historical (2021) and projected (2022–2032) ITRPV data on utility-scale module size [22].

agreement on uniform sizes for modules with 210-mm half-cut cells [37]. Projected module weight increases as well. About half of utility-scale modules weigh less than 25 kg in 2021, declining to 5% in 2032, at which time the remaining market share is split approximately evenly across modules weighing 25–30 kg and modules weighing 30–40 kg. Projected changes in residential module sizes are less dramatic, with the share of modules smaller than 1.8 m^2 declining from 49% in 2021 to 38% in 2032.

For the same module loading condition, cells within larger modules are more likely to fracture [38]. Thus, larger modules are potentially susceptible to more frequent cell breakage due to weather, shipping, handling, or installation. In addition, if larger modules produce higher electrical currents, electrical balance-of-system components (e.g., wire size, fuses, bypass diodes) must be modified appropriately.

Improving installation methods and mounting structure designs could mitigate reliability issues related to larger module sizes. One key may simply be proper workmanship, such as checking connections between frames and racks for wind loading, using the right fasteners and clips and installing them correctly, checking torque, and so forth [39], [40]. For utility-scale systems, issues related to transitioning from modules mounted at their edges (in fixed mounting structures) to their centers (in tracking structures) are exacerbated by using larger modules [35], [41]. Appropriate shipping techniques must be established for large modules, similar to how stacking moderately sized modules vertically instead of horizontally has mitigated the formation of microcracks during transportation [42]. However, reliability considerations established for smaller modules might not translate directly to larger modules. Hence, reliability tests and testing equipment must be modified to accommodate large modules, such as dynamic mechanical loading tests to assess wind loading and hail damage [31]. In addition, computational modeling can be a powerful tool for assessing scaling relationships [13]. Models validated for moderately sized models can be used in numerical studies to assess the implications of size increases on design parameters, such as module deflection, thermomechanical stresses, or material fatigue [43], [44], [45].

B. Larger Cells

Manufacturing advances have enabled the production of larger wafers and cells, which may help reduce PV installed
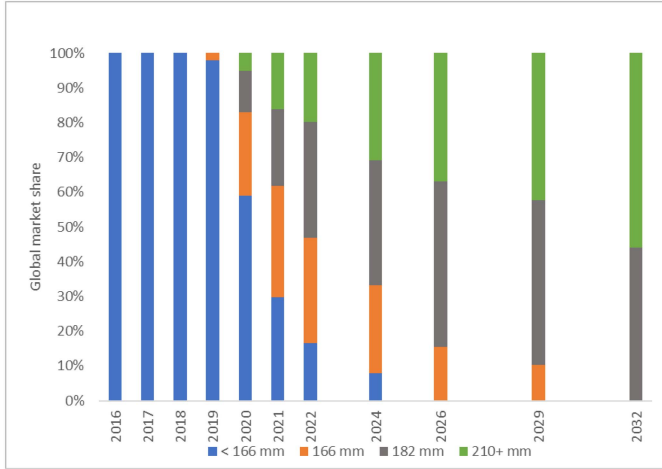
Fig. 4.   Historical (2016–2021) and projected (2022–2032) ITRPV data on Czochralski monocrystalline wafer size in mass production [17], [18], [19], [20], [21], [22].

Fig. 5.   Historical (2016–2021) and projected (2022–2032) ITRPV data on cell aspect ratios for wafer sizes of at least 182 mm × 182 mm [17], [18], [19], [20], [21], [22].

system costs by enabling higher module power [46] (see Section III-A). Larger wafers also provide efficiency benefits by enabling cell cutting [34], [47] (see Section III-C).

ITRPV historical estimates and projections show rapid growth of monocrystalline wafers larger than 166 mm × 166 mm (see Fig. 4). Wafer sizes of 182 mm × 182 mm and larger capture about 85% of the market share by 2026 and 100% by 2032. By comparison, InfoLink provides a more aggressive projection (not shown in the figure), reaching a 100% share of 182- and 210-mm wafers by 2025 [23].

Using larger wafers may increase the risk of damage during the handling, manufacturing, and packaging of large-format modules. Larger wafers are more susceptible to cracking than smaller wafers [38]. However, the most important reliability considerations relate to cell-cutting processes and the resulting cut-cell dimensions, which are discussed as follows.

C. Cell Cutting

Using cut cells reduces resistive losses in modules by lowering electric currents [48], [49], and it provides potentially higher shade tolerance [49], [50]. Full cells have largely disappeared for wafer sizes smaller than 182 mm × 182 mm, and they have completely disappeared for larger wafer sizes (see Fig. 5). Half cells are now the dominant configuration and are expected to remain so for the next decade.

From a reliability perspective, the smaller cells resulting from cutting are less susceptible to cracking than larger cells [38]. However, the cutting process introduces the potential for cell cracking due to defects along the cut edges [51], [52], [53].

The risk of cell damage can be reduced by optimizing the cutting process. Bosco et al. [53] demonstrated that an optimized cutting process can essentially eliminate cracked cells due to static and dynamic mechanical loading, compared with nonoptimized processes that result in significant cell cracking. Researchers have also demonstrated that cutting cells via thermal laser separation produces less damage than cutting them via laser scribing and cleavage [51], [52].
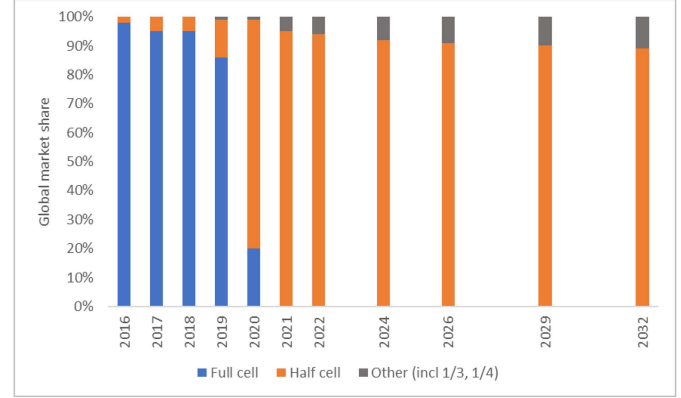
Once well-manufactured cut cells are laminated inside modules, they present a similar fracture risk compared with full cells [51]. In addition, recent research suggests that rotating cut cells 90° from their orientation in typical modules can reduce the probability of fracture further [54].

D. Thinner Cells

Making cells thinner reduces PV costs by reducing the amount of polysilicon used for the same amount of power capacity. During the 2009–2019 period, wafer thickness did not decrease as fast as the ITRPV predicted, possibly because of declining polysilicon prices and the greater resistance to breakage during packaging offered by wafers at least 180 μm thick [16], [17], [18], [22]. Industry instead introduced diamond wire sawing to reduce polysilicon consumption in wafer manufacturing via lower kerf loss. Starting in 2020, however, wafer thicknesses have dropped more significantly, likely due in part to the industry's desire to reduce polysilicon use further during a time of rising polysilicon prices [22]. ITRPV [22] states that reducing the as-cut wafer thickness is now becoming the "method of choice" for further polysilicon-related cost reductions, projecting thickness declines of 10%–20% between 2022 and 2032 (see Fig. 6). Current predictions associate the thinnest wafer forecasts with n-type cell architectures, which best exploit the efficiency gains possible from thin wafers (see Section VI).

Thinner silicon cells are more flexible and could allow for new curved module designs. However, there are concerns that thinner cells might be more susceptible to cracking than thicker cells. With decreasing wafer size, surface damage introduced by the sawing process can have a higher impact on fracture strength when compared to the sawing of thick wafers [55]. Similarly, wafer thickness reduction leads to higher sensitivity of the solar cell to mechanical loads, and optimization of the manufacturing and handling processes becomes necessary [56].

Because thinner cells are more difficult to handle during manufacturing, it is often assumed that their fracture risk is greater in general. However, thin cells might not be inherently more susceptible to cracking after they have been laminated inside a module. A holistic approach is required to address cell
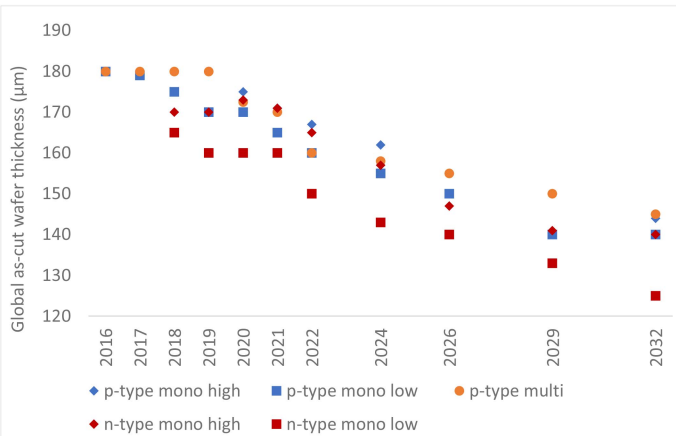
Fig. 6. Historical (2016–2021) and projected (2022–2032) ITRPV data on global as-cut wafer thickness [17], [18], [19], [20], [21], [22].

fracture risk, accounting for updated manufacturing processes, improved quality control, and overall PV module designs. In particular, multiple concurrent changes must be considered when assessing the fracture risk of thinner cells, such as changes to the interconnect technology, the stress localizations around those interconnects, the mechanical stress state and effective area of cells under tension, module packaging technology, edge-damage caused by the cutting process, cell thickness control, cell handling, as well as residual stresses caused by firing of the metallization and lamination process [33], [57]. Refined testing methods, improved models, and more research are needed to holistically address cell fracture risk and its implications for module design and power output.

IV. INTERCONNECT TECHNOLOGIES

We identified three main trends in interconnect technology: increased redundancy, geometry and process changes, and material changes. These individual trends are accompanied by an overarching trend of shrinking or eliminating the gap between cells to create high-energy-yield modules.

A. Increased Redundancy

Traditionally, the front-side metallization of a PV cell consists of grid fingers and busbars. The grid fingers are printed on the cell to collect the current generated by a fraction of the PV cell. Busbars are printed perpendicular to the grid fingers to collect the current from the fingers. Tabbing ribbons are then soldered onto the busbars, establishing the interconnection of cells within modules by connecting the front side of one cell to the back of the next. At the end of a cell string, a bus ribbon is used to connect the multiple tabbing ribbons together and wire them into the junction box. This traditional interconnect technology is shown at left in Fig. 7, where three tabbing ribbons are used to collect the current from the PV cell. The tabbing ribbons have rectangular cross sections and are typically made from copper and coated with a layer of solder to facilitate soldering. A cell using such an interconnect technology is typically referred to as a three-busbar cell.

Moving to the right in Fig. 7, interconnect technologies change from the traditional approach toward higher-energy-yield technologies. The second cell from the left uses five busbars, which decreases the distance between busbars and reduces resistance losses. Because the collected current is split into more busbars, the cross section of the tabbing ribbons and busbars becomes smaller, and shading losses are reduced. In the third cell, even more busbars are used, and the tabbing ribbon is replaced by a tabbing wire with a round cross section. In addition, the rectangular footprint of the busbar is changed to a dash-line pattern, which reduces the amount of metallization paste needed by using dedicated solder pads connected with a thin metallization strip. The fourth cell illustrates a "busbarless" approach. Here, the screen-printed busbars are omitted, and the tabbing wires are directly connected to the grid fingers (see Section IV-B for further details). Finally, shingled cells eliminate the gap between cells altogether, with cells overlapping each other by 1–2 mm and typically connected by electrically conductive adhesive (ECA). Shingled cell approaches can either use or omit busbars [58]; hence, we refer to shingling as zero-gap technology. We only use the term "busbarless" if there is no screen-printed metallization perpendicular to the grid fingers.

These trends are driven by several factors. As cells are getting larger, wider interconnection ribbons are required to conduct larger currents. However, the difference in coefficient of thermal expansion (CTE) of the ribbon and silicon wafer lead to a build-up of thermomechanical stresses that limits the possible cross-section size of the ribbon [59]. By including more busbars and interconnections, the individual ribbon size can be kept small, and the buildup of mechanical stresses can be reduced (see Section IV-B). More busbars and interconnections also enable reductions in cell finger width, which reduces costs by reducing silver metallization and increases efficiency by increasing the active cell area [60]. Finally, additional connections increase the likelihood of keeping fractured cell fragments electrically connected in the event of cell fracture, which increases reliability [61].

ITRPV projections show 9- to 10-busbar cells largely disappearing over the next decade, while the share of 11- to 12-busbar cells stays relatively constant and the shares with more than 12 busbars and no busbars increase (see Fig. 8). Note that these projections apply to M10 (182 mm × 182 mm) and larger cells; smaller cells may use fewer busbars.

On the risk side, the increase in the numbers of busbars has led to geometry, process, and material changes. Rectangular tabbing ribbons are being replaced by round tabbing wires in multiwire configurations, which can use conventional busbars, or busbarless approaches. The latter may introduce new processes and materials that can require the development of new tests and standards to assess long-term reliability [62]. Furthermore, tabbing ribbons or wires may be entirely replaced by new materials such as ECA that enable zero-gap configurations through shingling. These changes could adversely affect cell stresses, if not properly designed, and increase cell fracture risk as outlined in [63]. Sections IV-B and C discuss the geometry, process, and material changes in detail.
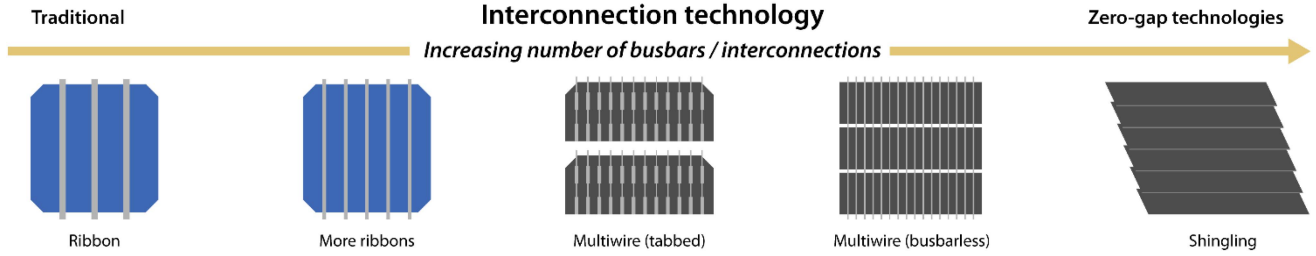
Fig. 7.   Evolution of interconnection technology from traditional ribbon bonding on polycrystalline cells (blue) to zero-gap shingling with monocrystalline cells (black). Grid fingers have been omitted for clarity (see Fig. 10 for details).
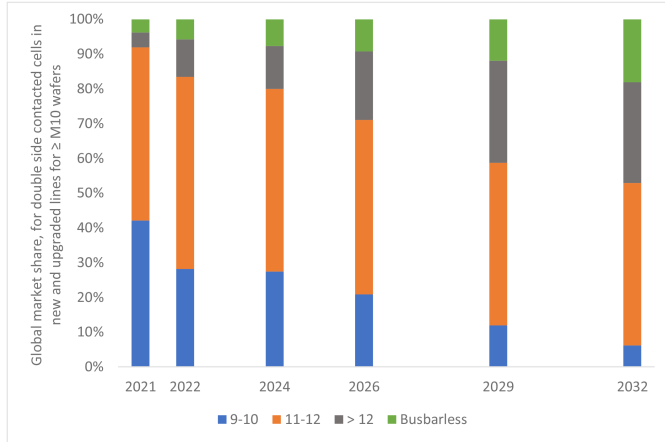

Fig. 8.   Historical (2021) and projected (2022–2032) ITRPV data on market shares by number of busbars, for double-side contacted cells in new and upgraded lines, and for wafers of M10 size (182 mm × 182 mm) and larger [22].
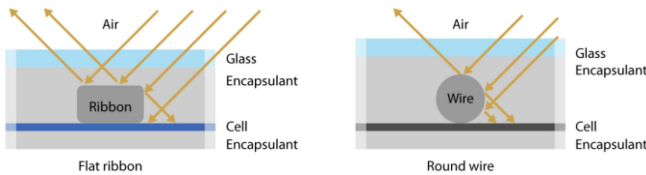

Fig. 9.   Geometry changes from flat ribbons (left) to round wires (right). The arrows illustrate the impact of the geometry on the incident light reaching the cell.

B. Geometry and Process Changes

Geometry changes in interconnect technologies can be observed in Fig. 7 by the narrowing of the flat ribbons from left to right, which eventually turn into wires and disappear in the case of shingled cells. Multiwire approaches [64], [65], [66], [67] improve efficiency by increasing the active cell area and leveraging light reflections off the wire. In Fig. 9, the impact on incident light is illustrated by changing from a flat ribbon (left) to a round wire interconnect (right). The round wire shades less of the cell and reflects more light down onto the cell. These benefits offset the efficiency loss caused by the additional shaded area due to more busbars. Ultimately, the shaded cell area is eliminated through zero-gap approaches such as shingling.

Fig. 10 shows process changes from a traditional tabbing process (left) toward a structured foil approach (right) [64]. Traditionally, a single print was used to create the front-side

metallization consisting of grid fingers and busbars, as indicated in the left-hand sketch in Fig. 10. Here, the electrical connection between the busbar and tabbing ribbon is established through soldering, which creates a metallurgical connection. A modification of this method is the so-called double-print process [68]. Here, a two-step screen print process is used to increase the height of grid fingers and busbars while decreasing their width, keeping the cross-sectional area constant. This process decreases shading losses by reducing the grid finger width [69] and covering the surface area of the front-side metallization. In the dual-print process, again a two-step process is used [70]. However, here the grid fingers are printed in the first step followed by a second step to add the busbars. Instead of using a simple rectangular shape for the busbars, as shown in the previous two processes, a dash-line pattern with dedicated solder pads is shown in the illustration, which depicts a more modern approach to reduce the material input required for the metallization [71]. Both tabbing ribbons and tabbing wires can be used with the dual-print process, and soldering is used to establish the electrical connection between the busbar and wire or ribbon. In contrast, the structured foil approach eliminates the soldering process by establishing an electrical connection directly between the tabbing wire and grid fingers. Dedicated busbars and soldering are omitted in this approach. Instead, the wires are embedded in a polymer foil and placed between the cells during the lamination process [64]. The electrical connections rely on establishing mechanical contact between the grid fingers and the low-temperature solder-coated tabbing wires during the lamination process (see Section IV-C for details and consequences of this technology change).

The changes in interconnect geometry and manufacturing processes are being driven by the efficiency benefits due to increasing the active cell area, reflecting more light onto the cell, and reducing or eliminating the gap between cells. In addition, the trend toward multiwire and shingling is driven by the need for low-temperature interconnect approaches. Structured foil and low-temperature solders lower the temperature requirements during the module packaging process and enable the use of new cell technologies, such as SHJ, that require lower processing temperatures after fabrication (see Section VI). Similarly, ECA can be cured at lamination temperature or below and is, therefore, suitable for temperature-sensitive technologies. ITRPV projections show round wires displacing flat ribbons over the next decade, with increased use of structured foil and shingled technologies as well (see Fig. 11).
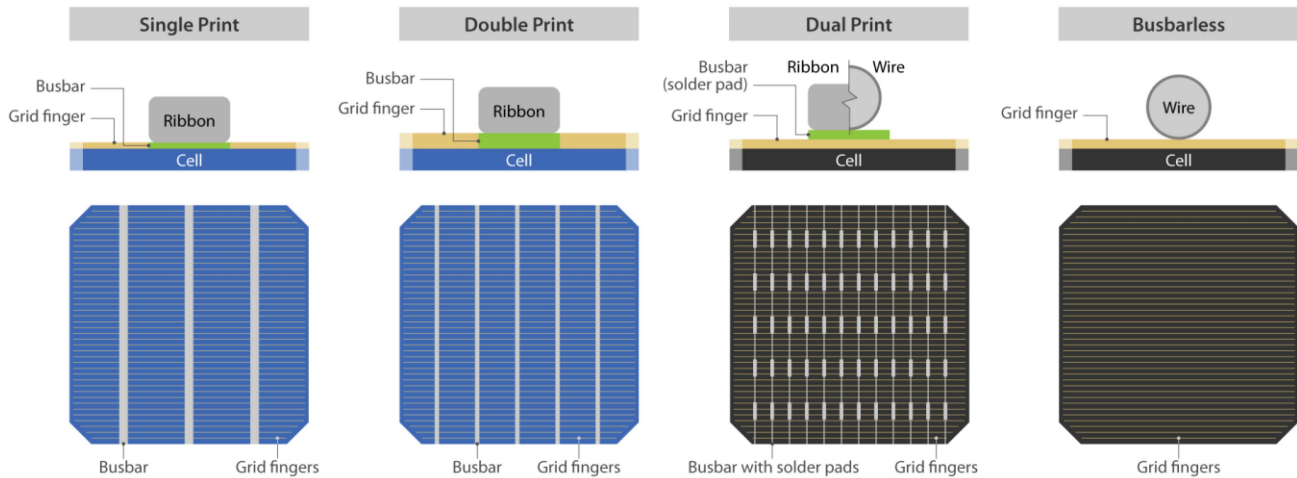
Fig. 10. Process changes. (a) Single print—a traditional tabbing process with few busbars and rectangular-shaped ribbons. (b) Double print—a modification of the traditional tabbing process to increase the metallization height, while decreasing the covered cell area. (c) Dual print—grid fingers and busbars are printed in separate steps, and in recent designs, more interconnects are used. (d) Busbarless—busbars are omitted, and only grid fingers are printed onto the cell.
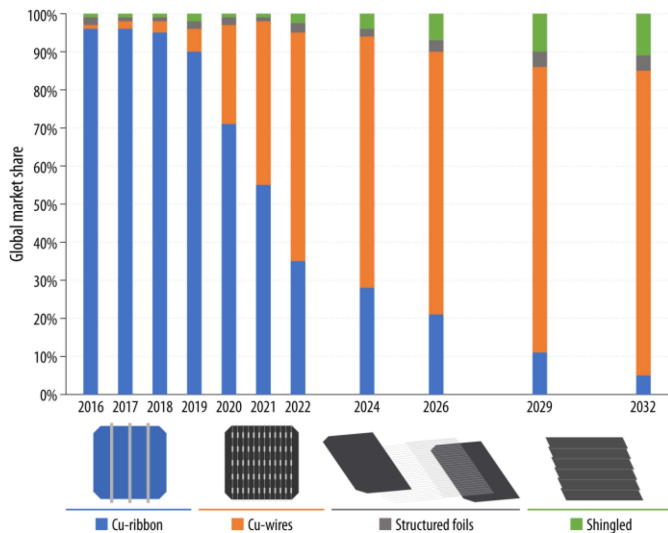

Fig. 11. Historical (2016–2021) and projected (2022–2032) ITRPV data on shares of interconnect technologies [17], [18], [19], [20], [21], [22]; structured foil diagram modified from [73].

Some of these changes can be incorporated easily into existing manufacturing processes (e.g., more busbars), but those requiring the introduction of new materials and processes require significant redesign of the entire PV module manufacturing and packaging process. Structured foil approaches, for example, introduce new manufacturing steps and require changes to adjacent packaging materials such as thicker encapsulants to accompany the round wires, which are thicker than flat ribbons. They further introduce new materials such as low-temperature solder alloys to establish a connection between the wire and the cell metallization, which introduces potential reliability risks. Similarly, shingled cell approaches significantly change the packaging process and the structural integrity of the whole module while introducing new materials such as ECA [72]. Current qualification standards such as IEC 61215 have not yet

been updated to account for all the emerging changes introduced in new module designs. Hence, additional research is necessary to assess whether the current standards are still sufficient to test modern PV module designs and materials, which are covered in the next section.

C. Interconnect Material Changes

Fig. 12 illustrates material changes, comparing traditional metallurgical connections versus emerging connections relying on mechanical contact to establish the electrical connectivity of the interconnect. As shown in the first two diagrams from the left, traditional metallurgical connections use conventional tin–lead (Sn–Pb) solders to bond ribbons and wires to the busbars across a wide contact area. In contrast, the last two diagrams show emerging interconnect technologies based on establishing a mechanical contact as the primary contacting mode instead of a metallurgical connection and incorporating new materials, such as low-temperature solders (In–Sn, Sn–Bi) or ECA. The first diagram in the mechanical contact category shows the structured foil technology described above. This technology eliminates busbars and a dedicated soldering process. Instead, electrical contact between the tabbing wire and grid finger is established during the lamination process. The tabbing wire is coated in a low-temperature solder that is intended to establish a metallurgical connection with the grid finger during lamination. However, thermomechanical fatigue resistance of low-temperature solders is generally poor when compared to conventional solders, and—coupled with the small contact area of this interconnect type—there is reason to believe that the primary contacting mode is not a metallurgical joint but rather a mechanical contact. Furthermore, Sn–Bi alloys were found to have thermal cycling acceleration factors of less than one, which may require accelerated testing protocols different from those used for conventional modules [62]. In the fourth diagram, an ECA—consisting of conductive particles in a polymer matrix—connects shingled cells directly without the need for an
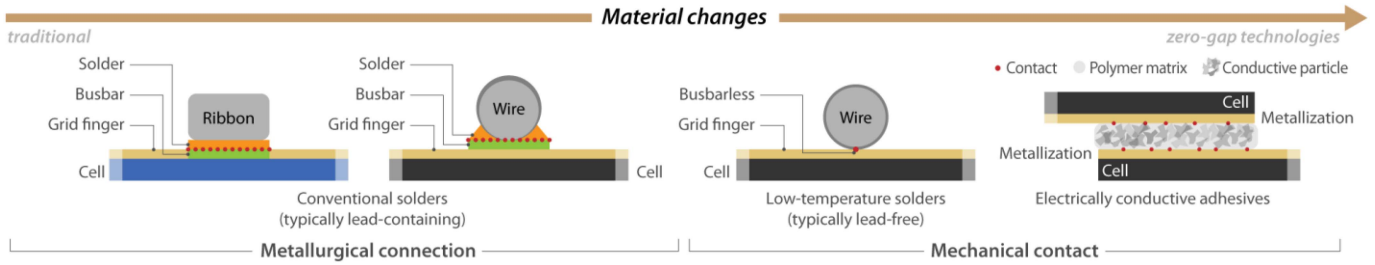
Fig. 12. Material changes related to interconnect technologies that use a metallurgical connection versus a mechanical contact to establish an electrical connection between tabbing ribbons or wires and the cell metallization.
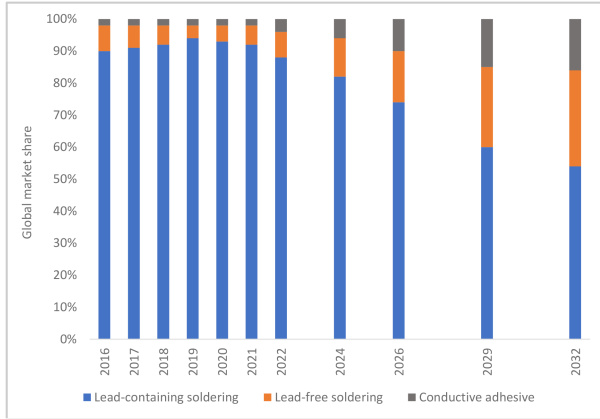

Fig. 13. Historical (2016–2021) and projected (2022–2032) ITRPV data on shares of interconnect materials [17], [18], [19], [20], [21], [22].

additional ribbon or wire. The electrical connection is created through shrinkage of the polymer matrix during curing, which causes the conductive particles to mechanically contact each other and establishes a conductive path.

Such material changes are being driven by the other interconnect trends discussed above but also by factors including regulatory restrictions on lead content in solders and the desire to cut costs by reducing silver use [74]. Additional drivers include the need to reduce cell stresses introduced during the soldering process [75] and to accommodate new cell technologies, such as SHJ, that require low-temperature interconnects [76].

ITRPV projections show a decrease in solders that contain lead and an increase in lead-free solders over time (see Fig. 13). Historically, conventional solders were associated with lead-containing solder such as Sn–Pb alloys, and lead-free solders were associated with low-temperature solders such as In–Sn or Sn–Bi alloys. However, this simplified distinction no longer holds true as solder advances are incorporating new materials into new alloys for conventional and low-temperature applications [77], [78]. Still, the ITRPV projections suggest a trend toward lead-free solutions with regard to solders and ECA.

On the risk side, new solder alloys might have different mechanical, metallurgical, and chemical characteristics compared with established materials, and new accelerated tests and standards will be needed to address the change away from metallurgical connections toward interconnects based on mechanical contact [65], [79]. For ECA, there are potential risks of new

degradation mechanisms such as debonding or corrosion of nonsilver conductive particles [45], [80], [81].

V. BIFACIAL

This section discusses technology trends and reliability implications related to bifacial modules, including the implications of using thinner glass, transparent backsheets, and encapsulants based on polyolefin elastomer (POE).

The market share of bifacial modules—typically with glass-glass configurations—has been increasing. Bifacial modules yield more power than monofacial modules because their cells are exposed to light on front and rear surfaces, which is effective for current p-type PERC cell technologies and is even more effective for emerging n-type technologies (see Section VI). Bifacial modules are used primarily in utility-scale systems [22] and are suitable for use on flat rooftops; typical sloped residential rooftop installations do not provide significant bifacial gain [82]. The proliferation of bifacial technologies has also been driven by the decreasing cost difference between monofacial and bifacial modules [83], [84], [85]. In the United States, an import tariff exemption has further enhanced the competitiveness of bifacial modules [82].

ITRPV [22] projections show the bifacial module market share increasing from 30% in 2022 to 60% in 2032, with most of those modules in a glass–glass configuration (see Fig. 14). Modules with front glass and transparent polymer backsheets, which are not specified here, could also play a role, depending on whether their cost premium over glass–glass modules decreases.

Bifacial module designs could experience new degradation and failure mechanisms that have not been present in traditional monofacial designs. For example, the greater weight of glass–glass modules is driving a trend toward thinner glass, but thinner glass presents potential reliability risks (see Section V-A). In addition, compared with glass-backsheet modules, glass–glass modules trap more of the acetic acid formed from the breakdown of encapsulants based on ethylene–vinyl acetate (EVA), which increases the risk of component corrosion. Using POE-based encapsulants, which do not degrade to form acetic acid, can mitigate this problem (see Section V-B).

A bifacial structure may also change typical module and cell degradation modes, including potential-induced degradation (PID) [86]. PID refers to several different mechanisms that result from the high potential difference between cells and the module frame during operation, and it can affect different cell
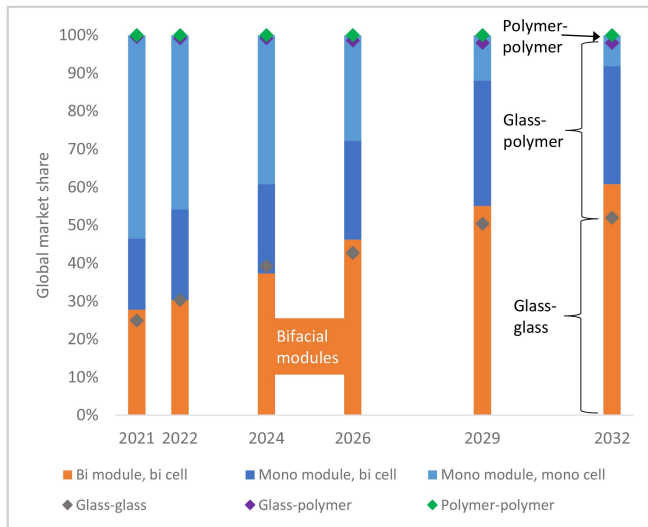
Fig. 14. Historical (2021) and projected (2022–2032) ITRPV data on bifacial and monofacial module, cell, and frontsheet–backsheet market shares [22].

Fig. 15. Historical (2017–2021) and projected (2022–2032) ITRPV data on module front and back glass thickness [18], [19], [20], [21], [22].

architectures differently (including bifacial versus monofacial PERC cells). It ultimately results in power losses, but it can be mitigated at the system, module, or cell level, and it is sometimes reversible in the field. See, for example, [87] for a review. Shunting-type PID (PID-s) occurs owing to the diffusion of ions, specifically Na^+, from the front glass into the cell, decreasing shunt resistance [87]. Additional PID mechanisms can occur on the rear side of bifacial cells and modules: degradation due to polarization of the cell surface (PID-p) [88], [89], [90] and corrosion of the silicon below the passivating layers PID (PIC-c) [90], [91]. Current PID testing (IEC 62804-1 ed. 1) is optimized for the monofacial configuration with the goal of detecting PID-s. However, performing only IEC 62804-1 ed. 1 may cause effects unique to bifacial modules to go undetected; updated PID testing for bifacial cells and modules should be considered [92]. Some PID mechanisms may be mitigated by encapsulant choice (see Section V-B).

Currently, there are contradictory results with respect to any difference in module operating temperature for glass–glass and glass–backsheet configurations [93], [94]. Higher operating temperatures are undesirable for two reasons. First, the increased temperature (reversibly) reduces power output by reducing cell efficiency [95]. Second, the increased temperature can accelerate irreversible degradation processes, risking module reliability [96]. Glass is a better thermal conductor compared to polymer backsheets and may dissipate heat more quickly, mitigating such concerns. Further studies are required to identify and validate whether glass–glass and glass–backsheet modules consistently run at similar temperatures.

Initially, glass–glass module designs were expected to reduce cell fracture risk by moving cells closer to the neutral axis of the PV laminate [96]. However, recent work suggests that glass–glass module designs may introduce higher residual stresses into the cells during the lamination process compared with traditional glass–backsheet designs [97], [98]. As the encapsulant contracts, a typical polymer backsheet can contract
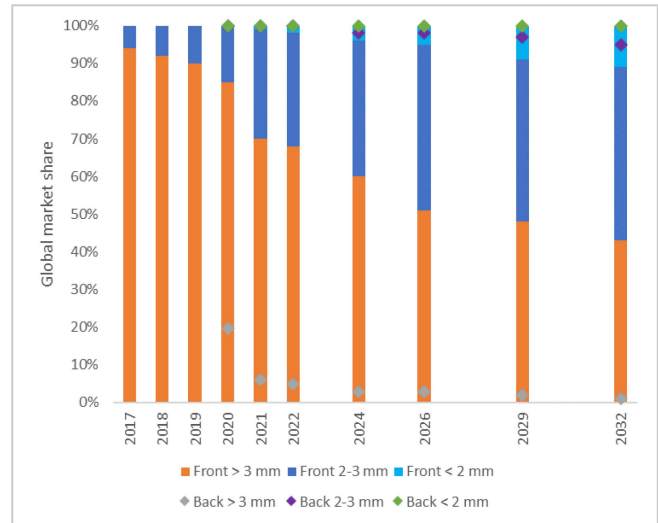
with it, minimizing stresses. However, a rigid glass layer does not contract as easily with the encapsulant, resulting in higher cell deflections and stresses around the ribbon-shaped tap wires. This mechanism is especially prominent in laminates using EVA-based encapsulants, leading to higher cell stresses compared with laminates using POE-based encapsulants. Changing from EVA- to POE-based encapsulant reduces the effect of residual stresses in glass–glass type constructions because the storage modulus and CTE for POE are lower than for EVA [98].

A. Thinner Glass and Transparent Backsheets

Making glass thinner than the standard 3.2 mm is one solution to the challenges presented by heavy, large bifacial modules. Thinner glass reduces transportation and installation costs, and it enhances solar transmittance. ITRPV projections show front glass thicker than 3 mm losing market share primarily to glass between 2 and 3 mm thick (see Fig. 15). The diamond symbols in Fig. 15 show the parallel trend for back glass thickness. Most back glass is already thinner than front glass, at 2 to 3 mm (see the area between the purple and gray diamonds), and it is projected to continue thinning over time.

Potential risks of thinner glass include reduced structural integrity and resistance to damage of modules from severe weather events and handling during installation. Thinner glass can also require a change in the heat treatment process. Tempered glass thinner than about 3 mm is not widely available owing to fabrication difficulties and high costs. Alternative treatments for thin glass—including heat strengthening and chemical toughening—affect the mechanical properties of the glass sheet [99]. Both heat-strengthened and tempered glass are treated through a high-temperature anneal followed by a quench, resulting in compressive stresses at the outer surface of the glass. The modulus of elasticity after the heat treatment remains unchanged, but the material strength increases proportionally to the rate of the quenching step. Tempered glass is quenched at a faster rate, which makes it stronger than heat-strengthened glass

and less likely to fracture, given the same dimensions [100]. In addition, changing from tempered to heat-strengthened glass changes the fracture pattern. Heat-strengthened glass fractures into much larger pieces, whereas tempered glass fractures into small pieces. Chemical toughening also induces compressive stresses at the outer surface of thin glass layers and increases the material strength, but its application is limited by high processing costs [101].

More testing and characterization are needed to better understand the reliability of using thin, heat-strengthened glass instead of thicker, tempered glass in modules [96]. Thinner, heat-strengthened glass with an inherently lower material strength will change the resistance of modules to hail impacts, although active mitigation options such as smart-stowing trackers could help prevent module damage from severe weather events [102]. Current hail testing procedures (ASTM E1038 and IEC 61215) might not be sufficient for the new locations in which PV is being deployed and might need to be updated with more representative hail information. Glass testing is further complicated by interactions with other module trends such as increasing module size (see Section III). Updated testing and standards are needed to appropriately account for thinner glass designs and should be carefully considered separately from other module variables.

Transparent polymer backsheets are another option for reducing the weight of bifacial modules [103]. Similar to traditional backsheets, transparent backsheets in bifacial modules offer corrosion resistance and easier manufacturing [96], [103], [104]. Smith et al. [104] demonstrated that transparent backsheets are appropriate for bifacial modules but care must be taken when designing the backsheet layers, particularly in relation to their susceptibility to UV degradation. Transparent polymer backsheets require additional accelerated and field testing to understand their long-term reliability [104].

B. Polyolefin-Based Encapsulants

Encapsulants are polymer materials that include many additives, including adhesion promoters, UV stabilizers, and so forth. Because of variability in composition and processing, encapsulant properties and reliability can vary widely by manufacturer. In this article, we compare "EVA-based encapsulants" with "POE-based encapsulants," but we acknowledge that the resulting generalizations may not hold true across all potential encapsulant formulations based on these materials.

The trend toward bifacial modules is contributing to the increased use of POE-based encapsulants and decreased use of EVA-based encapsulants. EVA is a semicrystalline copolymer of ethylene and 28%–33% vinyl acetate, with curing agents to induce crosslinking of the polymer chains during the lamination step [105]. EVA degrades in the presence of moisture to form acetic acid [106], [107], [108]. Acetic acid can typically escape a glass–polymer module through the permeable polymer backsheet [106]. However, in a glass–glass module, the acetic acid diffuses at a slower rate and may result in accelerated oxidation and corrosion of the interconnection and metallized layers [106], [109], [110], [111]. POE is also a semicrystalline copolymer, generally composed of a polyethylene backbone with different
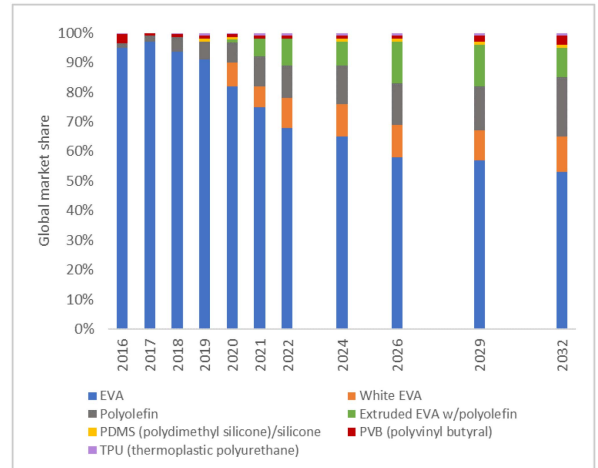

Fig. 16. Historical (2021) and projected (2022–2032) ITRPV data on encapsulant material market shares [17], [18], [19], [20], [21], [22].

side groups; it eliminates the acetic acid problem because it does not have a vinyl acetate side group and thus does not form acetic acid during degradation [113]. Moreover, POE-based encapsulants typically have a greater volume resistivity and lower water vapor transmission rate than EVA-based encapsulants, and these characteristics result in less PID [107], [112], [114], [115], [116], [117], [118], [119].

Factors hindering POE use include its higher cost and lower light transmission compared to EVA [120]. Still, ITRPV projections show the use of EVA-based encapsulants decreasing over time, while the shares of encapsulants based on POE and extruded EVA with POE increase up to about a third of the market within a decade (see Fig. 16).

Reliability risks associated with using POE in modules are largely associated with a lack of long-term durability testing. Such risks may be compounded by using POE with bills of materials optimized for EVA, which may affect the adhesion of the encapsulant to other components [107]. POE may also be associated with longer manufacturing times and narrower control windows for temperature, which might necessitate improved process and quality control. In addition, reliability risks might be introduced by manufacturing processes meant to reduce manufacturing costs. One such process is the use of mixed encapsulants (e.g., EVA in the front for lower cost and increased transmission and POE in the rear for reduced corrosion and PID), which might introduce new, unknown failure modes given the differences in material properties. Another process is the use of coextruded encapsulants, where a thinner layer of POE is sandwiched between two layers of EVA to reach the desired thickness [120]. The coextruded encapsulant reduces the lamination time and improves adhesion to glass [120]. However, understanding of the long-term reliability of this approach is limited by a lack of accelerated and field testing as well as a lack of known products using it. The recently published IEC TS 63209-2 is intended to provide a menu of tests to evaluate the long-term durability of polymeric materials and combinations of materials, and it would provide important data for evaluating new materials and module designs.
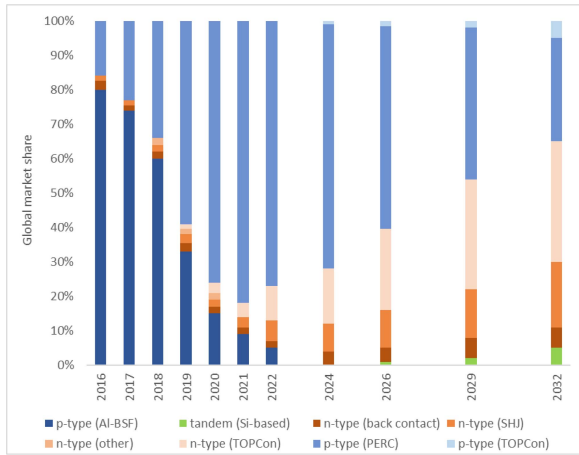
Fig. 17. Historical (2016–2021) and projected (2022–2032) ITRPV data on cell technologies (ITRPV cell categories reclassified by authors to highlight key trends) [17], [18], [19], [20], [21], [22].

VI. Cell Technology

Fig. 17 shows past and predicted cell transitions in terms of market share, synthesized from ITRPV. All silicon wafers are intentionally doped with impurity atoms to tune electronic properties: those doped with boron or gallium (electron acceptors in silicon) are called p-type, whereas wafers doped with phosphorus (an electron donor in silicon) are called n-type and have opposite polarity. Monocrystalline p-type PERC is the dominant silicon technology in 2022, having rapidly replaced p-type Al-BSF. ITRPV projects a transition toward n-type cells over the next decade, with n-type technologies achieving a market share of 60% in 2032 (see Fig. 17). PV Tech projects a faster transition, with n-type technologies achieving a market share of 90% by 2030 [15].

Fig. 18 shows cross-section schematics of the cell architectures discussed here. A recent review by Ballif et al. [121] addresses the improvements associated with these architectures. PERC cells improved upon Al-BSF by improving rear surface passivation, resulting in open-circuit voltage (VOC) gain from ~640 to ~680 mV in the best industrial devices of each type. Common PERC cell reliability issues include LID due to boron–oxygen defects, light- and elevated temperature-induced degradation (LETID), and PID (see Section V). Boron–oxygen LID reduces performance when susceptible cells are exposed to light but has been mitigated by a hydrogenation step [122], [123] and the transition away from boron-doped wafers, which produce the boron–oxygen defect, to gallium-doped wafers [124], [125]. From 2020 to 2022, gallium quickly supplanted boron as the dominant p-type dopant [20], [21], [22].

The transition to n-type is led by two cell architectures, shown in Fig. 18: TOPCon and SHJ. This transition is driven largely by enhanced efficiency stemming from the typically higher charge carrier lifetime of n-type monocrystalline silicon, which is best exploited when combined with TOPCon or SHJ architectures [126]. Also, these architectures are likely best optimized when applied on wafers thinner than the ~170 μm typical of PERC cells today, so they provide additional motivation to reduce wafer thickness [127], [128].

TOPCon cells have high efficiencies due to the physical separation of the rear metal layer from the bulk silicon by a tunnel oxide layer, which improves surface passivation and VOC up to approximately 720 mV. TOPCon cells have a higher bifaciality factor compared with PERC cells while using many of the same fundamental manufacturing processes, so industrial familiarity might promote TOPCon adoption. SHJ cells have high efficiencies due to superior surface passivation accomplished through intrinsic amorphous silicon layers, labeled "i-type a-Si" in the figure. This increases VOC as high as 750 mV, higher than TOPCon, while achieving very high bifaciality. On the other hand, SHJ has a substantially different manufacturing process compared with PERC or TOPCon, along with higher manufacturing equipment costs, which could hinder widespread introduction into the market.

Further n-type efficiency gains are possible with interdigitated back contact (IBC) cell structures (called "back contact" in Fig. 17), which combine the high-efficiency potential of n-type TOPCon or SHJ surface passivation while eliminating the self-shading of the front contacts [129]. IBC concepts have historically produced very high efficiencies in laboratories and factory production but commercially have been limited primarily to premium market segments (e.g., rooftop PV systems) owing to their high cost [130]. Relatively high projected costs limit the market shares of this technology, as shown in Fig. 17.

While the anticipated transition from gallium-doped p-type to n-type cells is primarily motivated by performance, n-type cells also offer reliability benefits, e.g., through lower LETID risk. LETID degrades performance when susceptible wafers are exposed to light at temperatures above ~50 °C, and it is caused at least in part by hydrogen in the silicon bulk. It can be mitigated via a number of factory approaches that essentially manipulate the quantity and chemical state of hydrogen in the cell [131]. LETID can occur in n-type wafers, but the risk seems to be reduced in n-type cell architectures, possibly due to reduced hydrogen introduced into the wafer bulk in n-type cell processing and/or other factors related to the precise processing history of the cells [131].

PID mechanisms need further investigation for n-type cells. As described in Section V, p-type PERC cells (particularly when bifacial) have been susceptible to several PID mechanisms; some of these have also been observed in some experiments on n-type cells. However, different n-type cell architectures exhibit different trends and susceptibility, and many open questions remain [132], [133]. Cells with a transparent conducting oxide (TCO) layer, such as typical SHJ cells, might be at risk of an additional corrosion-type PID mechanism, depending on their specific structure and the module architecture around them [134]. The risks of PID in n-type cells may not be any greater than in p-type cells in practice but more testing and study are necessary. An emphasis should be placed on understanding and mitigating PID risk in industrial implementations of the TOPCon and SHJ architectures, and standard PID tests specific to bifacial modules should be codified.

Cells based on high-lifetime n-type wafers in general have several more conceivable reliability risks. First, the high bulk lifetime of the wafer and the complexity of the surface
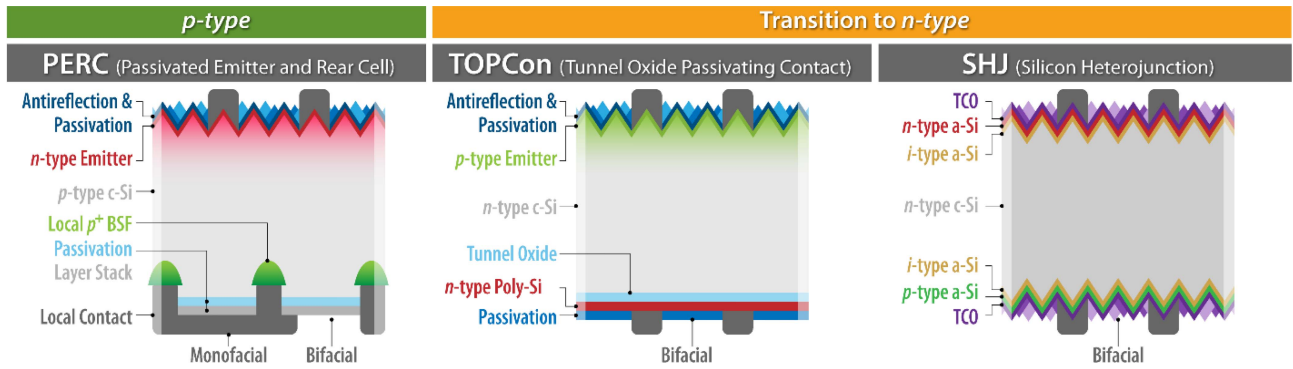
Fig. 18.   Cross-sectional schematics of PERC, TOPCon, and SHJ cell architectures.

layers multiply their sensitivities [121]. The performance of both TOPCon and SHJ relies critically on ultrathin and sophisticated surface passivation layers (tunnel oxide for TOPCon, a-Si-based layers for SHJ), which are an active area of global research and development. These layers could be susceptible to UV light-induced degradation, surface-related degradation, corrosion, or other as-yet unknown degradation modes, which would require testing and engineering to mitigate [135], [136], [137], [138], [139], [140]. Reliability testing of these cells may require new specific stress combinations and sequences [12]. Finally, n-type cells typically require higher silver content in their contacts compared to p-type cells, which increases costs, raises concerns about the global supply of silver, and motivates redesign of the metallization and interconnection scheme, as discussed previously [141]. Copper is an attractive alternative material owing to being both cheaper and more earth-abundant than silver, and SHJ has an additional requirement for low process temperature metallization and interconnection, which gives further motivation to replace silver. Plated copper metallization has been demonstrated in both TOPCon and SHJ cell architectures [142], [143], and copper-based screenprint pastes have been demonstrated on SHJ and IBC cells [144], [145]. Copper contacts could conceivably introduce new reliability issues, including increased risk of degradation from copper ingress into the cell and adhesion of plated contacts to the cell [146]. Plated copper might also require the adoption of new manufacturing processes and tools as well as different interconnection schemes [146]. On the other hand, some promising lab- and pilot-scale work has demonstrated equal or better performance by plated copper contacts in various reliability tests [143], [147], [148].

VII. DISCUSSION AND RECOMMENDATIONS

Our selected module technology trends have numerous, interrelated drivers and reliability implications. To give a few examples, more busbars and interconnections are needed to maintain performance in larger cells, and they improve reliability in larger, thinner cells because the cells are more likely to remain electrically connected if they crack. This interconnection trend has helped drive interconnection geometry, process, and material changes—including use of round wires in multiwire configurations and shingled cells connected by ECA—each of which has its own reliability benefits and risks. The trend toward multiwire and shingling with ECA is also driven by

the need for low-temperature interconnect approaches, related to the proliferation of n-type cells. The rise of high-efficiency n-type cells, with their high bifaciality factors, has a synergistic relationship with the rise of bifacial modules. The popularity of bifacial modules is driving the use of POE-based encapsulants (to mitigate corrosion risk) and thinner glass (to reduce weight but with potential implications for reliability, especially in increasingly large modules).

Individual technology changes have a range of potential effects on module reliability, from decreasing the risk of reliability problems, to having little or no impact, to increasing the risk. More important, and more complex, are the compounding effects of multiple concurrent changes. One prominent example is the significant increase in module area occurring simultaneously with the thinning of both wafers and cover glass plus, in some cases, the use of less-supportive framing and mounting—resulting in what many industry observers have informally dubbed "big floppy modules." This "big floppiness" from multiple changes likely increases the risk of mechanical damage more than the risk presented by any of the changes alone. A forward-looking evaluation of module reliability risks must account for the potential compound advantages and disadvantages of concurrent technology changes, which may in many cases be less intuitive than the example given here.

As our review shows, many reliability issues and mitigation strategies related to recent module technology trends have been at least partially characterized. For example, PID-s is a widely studied degradation mechanism for monofacial cells and modules, and increased rear-side PID-c and PID-p susceptibility in bifacial glass-glass technologies has been studied. However, recent work has highlighted the need for tailoring qualification tests to bifacial products, accounting for differences between bifacial PID and monofacial PID. Similar reasoning can be applied to all module material and technology changes. At a minimum, all changes should be assessed through established test procedures. The IEC retest guidelines (IEC TS 62915, implemented in 2018) require qualification retesting when significant module material or process changes are made. Such retesting subjects the new configurations to stresses known to induce failures in past products. Still, new failure mechanisms could arise owing to module changes or interactions within the bill of materials, and these new mechanisms may require new qualification standards and test procedures.

In general, our review highlights the ongoing need to assess the reliability implications of new module trends. For all new module technologies, it remains critical to collect and analyze long-term field data, although keeping up with rapid technological turnover is challenging, as discussed in Section I. Keeping standards and testing protocols aligned with emerging module designs and materials is similarly important yet difficult. Standards typically are developed to screen for known failure modes that have been observed in fielded modules. In this article, we note multiple examples of "new" failure modes that were missed by existing standards, including those related to AAA backsheets, hail damage, some PID modes, and cell-specific degradation modes such as LETID. The rapid pace of material and design evolution in PV cells and modules introduces multiple changes at once that may not be detected by tests developed for issues that have been seen before. Test protocols are needed to assess weaknesses without prior knowledge of the likely failure modes. The reliability community is constantly working to update testing protocols to test new materials and designs. For example, it is becoming more common to test for UV effects, larger hail, and so forth, even though these are not required by current standards.

We also identify research needs related to specific technology trends. For module architecture trends, research is needed to characterize the reliability implications of larger and thinner cells in conjunction with variations in module design, including interconnect type and thinner glass. Research and modified tests are required for assessing the effect of larger modules on cell cracking due to weather, shipping, handling, and installation. More broadly, a better understanding is needed for the multistep relationships between observable defects/cracks and long-term module degradation causing potential power loss.

For interconnection trends, research on potential new degradation mechanisms associated with ECA, such as debonding and corrosion of nonsilver conductive particles, would be valuable. In addition, existing tests and standards developed for traditional metallurgical interconnections might not be suitable for emerging technologies, such as structured foil approaches. The latter may be better characterized as using mechanical contact rather than metallurgical connection as the primary contacting mode. Thus, the associated reliability tests should be updated to account for this change.

For bifacial trends, the need for PID tests tailored to bifacial modules is mentioned above. In addition, accelerated and field testings are needed to assess the long-term reliability of mixed and coextruded encapsulants, and similar work is needed to assess the reliability of transparent polymer backsheets. Anecdotal reports based on fielded bifacial systems suggest that the transition to thinner glass increases reliability risks related to hail impacts. Hail testing may require modifications to account for more hail-prone PV system locations. Smart-stowing trackers could help prevent damage to bifacial modules using thinner glass. Furthermore, the structural integrity of modules with thinner glass might be reduced, which elevates the need for appropriate mounting and racking configurations to provide the necessary structural support to avoid glass breakage during severe weather events.

Fig. 19. PV reliability learning cycle, enabling continuous improvement to ensure quality despite ongoing technological changes.

Finally, for cell technology trends, there is a need to develop specific stress combinations and sequences for testing the reliability of n-type cells and their ultrathin surface passivation layers. In particular, testing and standards development are necessary to assess and screen for UV light-induced degradation and PID risk in industrial implementations of bifacial TOPCon and SHJ architectures.

We identified these research areas through our review and analysis at one point in time. We anticipate they will be useful to stakeholders in the near term. However, the evolution of PV module technology will be continuous, so the assessment of module reliability must be continuous as well. One way of conceptualizing a continuous improvement process is the PV reliability learning cycle shown in Fig. 19. The cycle employs several steps to maintain module quality in lockstep with technological change. In the first step of each trip through the cycle, introducing new products and designs produces anticipated and unanticipated effects within integrated modules. The remaining steps in the cycle represent the holistic reliability assessment needed to address the implications of these changes [6]. Field diagnostics are used to detect unexpected changes in module performance, followed by degradation and failure analysis to detect the root causes of the changes. The results of these analyses inform accelerated tests and standards development to account for new degradation mechanisms and detect any possible new failure modes in next-generation products. Currently, the industry relies on accelerated testing and standards to screen out previously observed failure modes and weaknesses. In the future, these tests and standards must add methods to detect and screen out unanticipated weaknesses and failure modes as well. Lifetime estimation and predictive modeling have the potential to enable the simultaneous assessment of multiple degradation mechanisms and their interactions through a unifying modeling framework [13]. Thus, lifetime estimation and predictive modeling complement field diagnostics, failure analysis, and accelerated testing to enable the detection and mitigation of

the unanticipated effects of new technologies before design changes are introduced into manufactured products. The PV reliability learning cycle begins again when findings from a previous cycle are incorporated into module performance and reliability improvements through new technological changes.

VIII. CONCLUSION

Maintaining the reliability of PV modules in the face of rapidly changing technology is critical to maximizing solar energy's contribution to global decarbonization. Our review helps identify potential future reliability risks before they become widespread in the market by linking emerging technology trends with their reliability implications. We leverage information and viewpoints from PV market reports, interviews with PV researchers and other industry stakeholders, and peer-reviewed literature to narrow the multitude of possible changes into a manageable set of 11 impactful trends likely to be incorporated in near-term crystalline-silicon module designs. We group the trends into four categories (module architecture, interconnect technologies, bifacial modules, and cell technology) and explore the drivers behind the changes, their interactions, and associated reliability risks.

Anticipating emerging technological changes in this way can help accelerate the PV reliability learning cycle. Our analysis identifies specific areas that would benefit from faster progress through the cycle, including needs for data collection, standards and test development, and research related to emerging module products and designs. Researchers should continue tracking module technologies and their reliability implications so efforts can be focused on the most impactful trends. As the rapid technological evolution continues, it is also critical to incorporate fundamental knowledge into models that can predict module reliability. Predictive capabilities complete the PV reliability learning cycle—reducing the time required to assess new designs and mitigating the risks associated with large-scale deployment of new products. Thus, getting ahead of the curve on module reliability will help ensure that PV continues to play a central role in the global energy transition.

REFERENCES

[1] Int. Energy Agency, "Net zero by 2050: A roadmap for the global energy sector," Int. Energy Agency, Paris, France, 2021. [Online]. Available: https://iea.blob.core.windows.net/assets/deebef5d-0c34-4539-9d0c-10b13d840027/NetZeroby2050-ARoadmapfortheGlobalEnergySector_CORR.pdf

[2] H. Mirletz, S. Ovaitt, S. Sridhar, and T. M. Barnes, "Circular economy priorities for photovoltaics in the energy transition," *PLoS One*, vol. 17, no. 9, Sep. 2022, Art. no. e0274351, doi: 10.1371/journal.pone.0274351.

[3] I. M. Peters, J. Hauch, C. Brabec, and P. Sinha, "The value of stability in photovoltaics," *Joule*, vol. 5, no. 12, pp. 3137–3153, Dec. 2021, doi: 10.1016/j.joule.2021.10.019.

[4] D. Jordan, T. Barnes, N. Haegel, and I. Repins, "Build solar-energy systems to last—Save billions," *Nature*, vol. 600, no. 7888, pp. 215–217, Dec. 2021, doi: 10.1038/d41586-021-03626-9.

[5] M. Theristis et al., "Onymous early-life performance degradation analysis of recent photovoltaic module technologies," *Prog. Photovolt.*, vol. 31, pp. 149–160, Aug. 2022, doi: 10.1002/pip.3615.

[6] D. C. Jordan, N. Haegel, and T. M. Barnes, "Photovoltaics module reliability for the terawatt age," *Prog. Energy*, vol. 4, no. 2, Apr. 2022, Art. no. 022002, doi: 10.1088/2516-1083/ac6111.

[7] L. Stoker, "PV Talks: PVEL's Tristan Erion-Lorico on 2022's solar module performance trends," PV Tech, May 31, 2022. [Online]. Available: https://www.pv-tech.org/pv-talks-pvels-tristan-erion-lorico-on-2022s-solar-module-performance-trends/

[8] M. Aghaei et al., "Review of degradation and failure phenomena in photovoltaic modules," *Renewable Sustain. Energy Rev.*, vol. 159, May 2022, Art. no. 112160, doi: 10.1016/j.rser.2022.112160.

[9] A. Fischer, "Maxeon 40-year solar panel warranty available in select markets," PV Mag., Feb. 4, 2022. [Online]. Available: https://pv-magazine-USA.com/2022/02/04/maxeon-40-year-solar-panel-warranty-available-in-select-markets/

[10] U.S. Dept. Energy, "SETO FY21—Photovoltaics," 2022. [Online]. Available: https://www.energy.gov/eere/solar/seto-fy21-photovoltaics

[11] J. Kim et al., "A review of the degradation of photovoltaic modules for life expectancy," *Energies*, vol. 14, no. 14, Jan. 2021, Art. no. 4278, doi: 10.3390/en14144278.

[12] M. Owen-Bellini et al., "Advancing reliability assessments of photovoltaic modules and materials using combined-accelerated stress testing," *Prog. Photovolt. Res. Appl.*, vol. 29, no. 1, pp. 64–82, Jan. 2021, doi: 10.1002/pip.3342.

[13] M. Springer, D. C. Jordan, and T. M. Barnes, "Future-proofing photovoltaics module reliability through a unifying predictive modeling framework," *Prog. Photovolt., Res. Appl.*, vol. 31, pp. 546–553, 2022.

[14] P. Basore and D. Feldman, "Solar photovoltaics: Supply chain deep dive assessment," U.S. Dept. Energy, Washington, DC, USA, DOE/OP-0012, 2022. [Online]. Available: https://www.energy.gov/sites/default/files/2022-02/Solar%20Energy%20Supply%20Chain%20Report%20-%20Final.pdf

[15] L. Stoker, "The race to the TOPCon," PV Tech Power, Nov. 2021. [Online]. Available: http://www.pv-tech.org/power

[16] ITRPV, *International Technology Roadmap for Photovoltaic (ITRPV): 2015 Results*, 7th ed. Frankfurt, Germany: VDMA, 2016.

[17] ITRPV, *International Technology Roadmap for Photovoltaic (ITRPV): 2016 Results*, 8th ed. Frankfurt, Germany: VDMA, 2017.

[18] ITRPV, *International Technology Roadmap for Photovoltaic (ITRPV): 2017 Results*, 9th ed. Frankfurt, Germany: VDMA, 2018.

[19] ITRPV, *International Technology Roadmap for Photovoltaic (ITRPV): 2018 Results*, 10th ed. Frankfurt, Germany: VDMA, 2019.

[20] ITRPV, *International Technology Roadmap for Photovoltaic (ITRPV): 2019 Results*, 11th ed. Frankfurt, Germany: VDMA, 2020.

[21] ITRPV, *International Technology Roadmap for Photovoltaic (ITRPV): 2020 Results*, 12th ed. Frankfurt, Germany: VDMA, 2021.

[22] ITRPV, *International Technology Roadmap for Photovoltaic (ITRPV): 2021 Results*, 13th ed. Frankfurt, Germany: VDMA, 2022.

[23] InfoLink Consulting, "Forecast for market share by wafer size," 2022. [Online]. Available: https://www.infolink-group.com/

[24] InfoLink Consulting, "N-type module: Capacity and shipment (2020–2025)," 2022. [Online]. Available: https://www.infolink-group.com

[25] M. Mittag and M. Ebert, "Systematic PV-module optimization with the cell-to-module (CTM) analysis software," *Sol. Cells*, vol. 4, p. 585, 2014.

[26] H. Yousuf et al., "Cell-to-module simulation analysis for optimizing the efficiency and power of the photovoltaic module," *Energies*, vol. 15, no. 3, Jan. 2022, Art. no. 1176, doi: 10.3390/en15031176.

[27] E. Urrejola et al., "*BifiPV2020 Bifacial Workshop: A Technology Overview*. Golden, CO, USA: Nat. Renewable Energy Lab., NREL/TP-5K00-77817, 2020, doi: 10.2172/1710156.

[28] P. Baliozian et al., "The international technology roadmap for photovoltaics and the significance of its decade-long projections," in *Proc. 37th Eur. PV Sol. Energy Conf. Exhib.*, 2020, pp. 7–11.

[29] M. Dhimish, V. Holmes, B. Mehrdadi, and M. Dales, "The impact of cracks on photovoltaic power performance," *J. Sci., Adv. Mater. Devices*, vol. 2, no. 2, pp. 199–209, Jun. 2017, doi: 10.1016/j.jsamd.2017.05.005.

[30] M. Köntges, I. Kunze, S. Kajari-Schröder, X. Breitenmoser, and B. Bjørneklett, "Quantifying the risk of power loss in PV modules due to micro cracks," in *Proc. 25th Eur. Photovolt. Sol. Energy Conf.*, 2010, pp. 3745–3752.

[31] T. J. Silverman, N. Bosco, M. Owen-Bellini, C. Libby, and M. G. Deceglie, "Millions of small pressure cycles drive damage in cracked solar cells," *IEEE J. Photovolt.*, vol. 12, no. 4, pp. 1090–1093, Jul. 2022, doi: 10.1109/JPHOTOV.2022.3177139.

[32] M. Mathusuthanan, M. Gembali, K. R. Narayanan, and K. Jayabal, "Analysis of micro-cracks evolution in silicon cell during entire solar photovoltaic module manufacturing process," *Sol. Energy*, vol. 224, pp. 1160–1169, Aug. 2021, doi: 10.1016/j.solener.2021.06.075.

[33] L. Papargyri et al., "Modelling and experimental investigations of micro-cracks in crystalline silicon photovoltaics: A review," *Renewable Energy*, vol. 145, pp. 2387–2408, Jan. 2020, doi: 10.1016/j.renene.2019.07.138.

[34] S. Chunduri and M. Schmela, *Advanced Module Technologies, 2021 Edition*. Düsseldorf, Germany: TaiyangNews, 2021.

[35] T. Sylvia, "Large format modules present a new set of challenges," PV Mag. Int., 2021. Accessed: Sep. 9, 2022. [Online]. Available: https://www.pv-magazine.com/2021/10/27/large-format-modules-present-a-new-set-of-challenges/

[36] T. Sylvia, "The opportunities and challenges presented by large-format modules," PV Mag., Mar. 3, 2022. [Online]. Available: https://pv-magazine-USA.com/2022/03/03/the-opportunities-and-challenges-presented-by-large-format-modules/

[37] Trina Solar, "Standardization of 210mm-size modules significantly boosts the PV industrial chain and system value," Trina Solar, 2021. Accessed: Sep. 29, 2022. [Online]. Available: https://www.trinasolar.com/en-glb/resources/newsroom/mastandardization-210mm-size-modules-significantly-boosts-pv-industrial-chain-and

[38] N. Bosco, M. Springer, J. Liu, S. N. Venkat, and R. H. French, "Employing Weibull analysis and weakest link theory to resolve crystalline silicon PV Cell strength between bare cells and reduced- and full-sized modules," *IEEE J. Photovolt.*, vol. 11, no. 3, pp. 731–741, May 2021, doi: 10.1109/JPHOTOV.2021.3056673.

[39] C. Doyle et al., *Solar Access to Public Capital (SAPC) Working Group: Best Practices in PV System Installation, Version 1.0*. Golden, CO, USA: Nat. Renewable Energy Lab., NREL/SR-6A20-63234, 2015.

[40] Nat. Renewable Energy Lab., Sandia Nat. Lab., SunSpec Alliance, and SunShot Nat. Lab. Multiyear Partnership (SuNLaMP) PV O&M Best Practices Working Group, *Best Practices for Operation and Maintenance of Photovoltaic and Energy Storage Systems*, 3rd ed. Golden, CO, USA: Nat. Renewable Energy Lab., NREL/TP-7A40-7382, 2018.

[41] E. Young, X. He, R. King, and D. Corbus, "A fluid-structure interaction solver for investigating torsional galloping in solar-tracking photovoltaic panel arrays," *J. Renewable Sustain. Energy*, vol. 12, no. 6, Nov. 2020, Art. no. 063503, doi: 10.1063/5.0023757.

[42] M. Köntges et al., "Impact of transportation on silicon wafer-based photovoltaic modules," *Prog. Photovolt., Res. Appl.*, vol. 24, no. 8, pp. 1085–1095, 2016, doi: 10.1002/pip.2768.

[43] J. Y. Hartley et al., "Effects of photovoltaic module materials and design on module deformation under load," *IEEE J. Photovolt.*, vol. 10, no. 3, pp. 838–843, May 2020, doi: 10.1109/JPHOTOV.2020.2971139.

[44] A. J. Beinert et al., "The effect of cell and module dimensions on thermomechanical stress in PV modules," *IEEE J. Photovolt.*, vol. 10, no. 1, pp. 70–77, Jan. 2020, doi: 10.1109/JPHOTOV.2019.2949875.

[45] M. Springer and N. Bosco, "Environmental influence on cracking and debonding of electrically conductive adhesives," *Eng. Fracture Mechanics*, vol. 241, Jan. 2021, Art. no. 107398, doi: 10.1016/j.engfracmech.2020.107398.

[46] S. Chunduri and M. Schmela, *Advantages of 210mm Solar Modules*. Düsseldorf, Germany: TaiyangNews, 2021.

[47] S. Guo et al., "Investigation of the short-circuit current increase for PV modules using halved silicon wafer solar cells," *Sol. Energy Mater. Sol. Cells*, vol. 133, pp. 240–247, Feb. 2015, doi: 10.1016/j.solmat.2014.11.012.

[48] S. Guo, J. P. Singh, I. M. Peters, A. G. Aberle, and T. M. Walsh, "A quantitative analysis of photovoltaic modules using halved cells," *Int. J. Photoenergy*, vol. 2013, pp. 1–8, 2013, doi: 10.1155/2013/739374.

[49] D. W. Cunningham et al., "Reaching grid parity using BP solar crystalline silicon technology," in *Proc. 35th IEEE Photovolt. Spec. Conf.*, 2010, pp. 1197–1202. doi: 10.1109/PVSC.2010.5614084.

[50] A. Calcabrini, R. Weegink, P. Manganiello, M. Zeman, and O. Isabella, "Simulation study of the electrical yield of various PV module topologies in partially shaded urban scenarios," *Sol. Energy*, vol. 225, pp. 726–733, Sep. 2021, doi: 10.1016/j.solener.2021.07.061.

[51] F. Kaule et al., "Mechanical damage of half-cell cutting technologies in solar cells and module laminates," presented at the SILICONPV, 8th Int. Conf. Crystalline Silicon Photovolt., Lausanne, Switzerland, 2018, Art. no. 020013, doi: 10.1063/1.5049252.

[52] C. Zhang et al., "Influence of laser condition on the electrical and mechanical performance of bifacial half-cutting PERC solar cell and module," *Int. J. Energy Res.*, vol. 46, pp. 15290–15299, Jun. 2022, doi: 10.1002/er.8229.

[53] N. Bosco et al., "Employing fracture statistics to track cell reliability through module fabrication," presented at the 47th IEEE Photovolt. Spec. Conf., 2020, pp. 263–265.

[54] N. Bosco, "Turn your half-cut cells for a stronger module," *IEEE J. Photovolt.*, vol. 12, no. 5, pp. 1149–1153, Sep. 2022, doi: 10.1109/JPHOTOV.2022.3192118.

[55] H. Sekhar et al., "Mechanical strength problem of thin silicon wafers (120 and 140 μm) cut with thinner diamond wires (Si kerf $120 \to 100$ μm) for photovoltaic use," *Mater. Sci. Semicond. Process.*, vol. 119, Nov. 2020, Art. no. 105209, doi: 10.1016/j.mssp.2020.105209.

[56] S. Pingel, Y. Zemen, O. Frank, T. Geipel, and J. Berghold, "Mechanical stability of solar cells within solar panels," in *Proc. 24th Eur. Photovolt. Sol. Energy Conf.*, 2009, vol. 21/25, p. 5, doi: 10.4229/24THE-UPVSEC2009-4AV.3.49.

[57] M. W. Akram et al., "Study of manufacturing and hotspot formation in cut cell and full cell PV modules," *Sol. Energy*, vol. 203, pp. 247–259, Jun. 2020, doi: 10.1016/j.solener.2020.04.052.

[58] W. Oh, H. Jee, J. Bae, and J. Lee, "Busbar-free electrode patterns of crystalline silicon solar cells for high density shingled photovoltaic module," *Sol. Energy Mater. Sol. Cells*, vol. 243, Aug. 2022, Art. no. 111802, doi: 10.1016/j.solmat.2022.111802.

[59] M. T. Zarmai, N. N. Ekere, C. F. Oduoza, and E. H. Amalu, "A review of interconnection technologies for improved crystalline silicon solar cell photovoltaic module assembly," *Appl. Energy*, vol. 154, pp. 173–182, Sep. 2015, doi: 10.1016/j.apenergy.2015.04.120.

[60] J. Walter, M. Tranitz, M. Volk, C. Ebert, and U. Eitner, "Multi-wire interconnection of busbar-free solar cells," *Energy Procedia*, vol. 55, pp. 380–388, Jan. 2014, doi: 10.1016/j.egypro.2014.08.109.

[61] T. J. Silverman et al., "Movement of cracked silicon solar cells during module temperature changes," in *Proc. IEEE 46th Photovolt. Spec. Conf.*, 2019, pp. 1517–1520, doi: 10.1109/PVSC40753.2019.8981150.

[62] L. Spinella and N. Bosco, "Thermomechanical fatigue resistance of low temperature solder for multiwire interconnects in photovoltaic modules," *Sol. Energy Mater. Sol. Cells*, vol. 225, Jun. 2021, Art. no. 111054, doi: 10.1016/j.solmat.2021.111054.

[63] N. Klasen et al., "Root cause analysis of solar cell cracks at shingle joints," *Sol. Energy Mater. Sol. Cells*, vol. 238, May 2022, Art. no. 111590, doi: 10.1016/j.solmat.2022.111590.

[64] C. Ballif et al., "SmartWire solar cell interconnection technology," in *Proc. 29th Eur. Photovolt. Sol. Energy Conf. Exhib.*, 2014, pp. 2555–2561, doi: 10.4229/EUPVSEC20142014-5DO.16.3.

[65] L. Spinella et al., "Reliability implications of solder in multiwire modules under dynamic mechanical loading," in *Proc. IEEE 48th Photovolt. Spec. Conf.*, 2021, pp. 108–111. doi: 10.1109/PVSC43889.2021.9518566.

[66] T. Söderström et al., "Low cost high energy yield solar module lines and its applications," in *Proc. IEEE 42nd Photovolt. Spec. Conf.*, 2015, pp. 1–6, doi: 10.1109/PVSC.2015.7356431.

[67] J. Govaerts et al., "Encapsulant-integrated interconnection of bifacial solar cells for BIPV applications: Latest results in the TWILL-BIPV project," in *Proc. EU PVSEC*, Oct. 2020, pp. 33–37, doi: 10.4229/EU-PVSEC20202020-1AO.3.3.

[68] M. Galiazzo, V. Furin, D. Tonini, G. Cellere, and A. Baccini, "Double printing of front contact Ag in C-Si solar cells," in *Proc. 25th Eur. Photovolt. Sol. Energy Conf.*, 2010.

[69] T. Wenzel et al., "Progress with screen printed metallization of silicon solar cells—Towards 20 μm line width and 20 mg silver laydown for PERC front side contacts," *Sol. Energy Mater. Sol. Cells*, vol. 244, Aug. 2022, Art. no. 111804, doi: 10.1016/j.solmat.2022.111804.

[70] H. Hannebauer, T. Dullweber, T. Falcon, X. Chen, and R. Brendel, "Record low Ag paste consumption of 67.7 mg with dual print," *Energy Procedia*, vol. 43, pp. 66–71, Jan. 2013, doi: 10.1016/j.egypro.2013.11.089.

[71] K. L. Ho et al., "The influence of cell busbar pattern on PV module reliability," in *Proc. 29th Eur. Photovolt. Sol. Energy Conf. Exhib.*, 2014, pp. 2562–2565, doi: 10.4229/EUPVSEC20142014-5DO.16.4.

[72] B. Litzenburger et al., "Innovative and gentle interconnection technique for high efficiency c-Si solar cells and cost-of-ownership-analysis (COO)," in *Proc. 26th Eur. Photovolt. Sol. Energy Conf. Exhib.*, 2011, pp. 3125–3132, doi: 10.4229/26thEUPVSEC2011-4CO.6.4.

[73] SolarTech Universal, "Smart wire connection technology," 2022. [Online]. Available: https://www.solartechuniversal.com/smartwire-technology

[74] D. Güldali and A. D. Rose, "Material joint analysis of lead-free interconnection technologies for silicon photovoltaics," in *Proc. 45th Int. Spring Seminar Electron. Technol.*, 2022, pp. 1–8, doi: 10.1109/ISSE54558.2022.9812798.

[75] A. J. Beinert et al., "Enabling the measurement of thermomechanical stress in solar cells and PV modules by confocal micro-Raman spectroscopy," *Sol. Energy Mater. Sol. Cells*, vol. 193, pp. 351–360, May 2019, doi: 10.1016/j.solmat.2019.01.028.

[76] Y. Zeng et al., "Review on metallization approaches for high-efficiency silicon heterojunction solar cells," *Trans. Tianjin Univ.*, vol. 28, no. 5, pp. 358–373, Oct. 2022, doi: 10.1007/s12209-022-00336-9.

[77] P. Schmitt, P. Kaiser, C. Savio, M. Tranitz, and U. Eitner, "Intermetallic phase growth and reliability of SN-AG-soldered solar cell joints," *Energy Procedia*, vol. 27, pp. 664–669, Jan. 2012, doi: 10.1016/j.egypro.2012.07.126.

[78] T. Geipel, D. Eberlein, and A. Kraft, "Lead-free solders for ribbon interconnection of crystalline silicon PERC solar cells with infrared soldering," *Amer. Inst. Phys. Conf. Proc.*, vol. 2156, no. 1, Sep. 2019, Art. no. 020015, doi: 10.1063/1.5125880.

[79] A. Fairbrother, L. Gnocchi, C. Ballif, and A. Virtuani, "Corrosion testing of solar cells: Wear-out degradation behavior," *Sol. Energy Mater. Sol. Cells*, vol. 248, Dec. 2022, Art. no. 111974, doi: 10.1016/j.solmat.2022.111974.

[80] M. Springer and N. Bosco, "Linear viscoelastic characterization of electrically conductive adhesives used as interconnect in photovoltaic modules," *Prog. Photovolt., Res. Appl.*, vol. 28, no. 7, pp. 659–681, 2020, doi: 10.1002/pip.3257.

[81] X. M. Zhang, X.-L. Yang, and B. Wang, "Electrical properties of electrically conductive adhesives from epoxy and silver-coated copper powders after sintering and thermal aging," *Int. J. Adhesion Adhesives*, vol. 105, Mar. 2021, Art. no. 102785, doi: 10.1016/j.ijadhadh.2020.102785.

[82] D. Feldman et al., "Spring 2022 solar industry update (national renewable energy laboratory)," presented at the Nat. Renewable Energy Lab., Golden, CO, USA, Apr. 26, 2022.

[83] C. Deline, S. A. Pelaez, B. Marion, M. Woodhouse, and J. Stein, "Bifacial PV system performance: Separating fact from fiction (PVSC 46, Chicago)," presented at the Photovolt. Spec. Conf., Chicago, IL, USA, 2019.

[84] C. D. Rodríguez-Gallegos et al., "Monofacial vs bifacial Si-based PV modules: Which one is more cost-effective?," *Sol. Energy*, vol. 176, pp. 412–438, Dec. 2018, doi: 10.1016/j.solener.2018.10.012.

[85] C. D. Rodríguez-Gallegos et al., "Global techno-economic performance of bifacial and tracking photovoltaic systems," *Joule*, vol. 4, no. 7, pp. 1514–1541, Jul. 2020, doi: 10.1016/j.joule.2020.05.005.

[86] P. Hacke et al., "Evaluation of bifacial module technologies with combined-accelerated stress testing," *Prog. Photovolt.*, vol. 31, pp. 1270–1284, 2023, doi: 10.1002/pip.3636.

[87] W. Luo et al., "Potential-induced degradation in photovoltaic modules: A critical review," *Energy Environ. Sci.*, vol. 10, pp. 43–68, 2017, doi: 10.1039/c6ee02271e.

[88] R. Swanson et al., "The surface polarization effect in high-efficiency silicon solar cells," in *Proc. 15th Int. Photovolt. Sol. Energy Conf. Exhib.*, 2005, pp. 410–413.

[89] S. Yamaguchi, K. Nakamura, A. Masuda, and K. Ohdaira, "Rapid progression and subsequent saturation of polarization-type potential-induced degradation of n-type front-emitter crystalline-silicon photovoltaic modules," *Jpn. J. Appl. Phys.*, vol. 57, no. 12, Nov. 2018, Art. no. 122301.

[90] K. Sporleder et al., "Quick test for reversible and irreversible PID of bifacial PERC solar cells," *Sol. Energy Mater. Sol. Cells*, vol. 219, 2021, Art. no. 110755, doi: 10.1016/j.solmat.2020.110755.

[91] K. Sporleder et al., "Local corrosion of silicon as root cause for potential-induced degradation at the rear side of bifacial PERC solar cells," *Phys. Status Solidi Regional Res. Lab.*, vol. 13, no. 9, Sep. 2019, Art. no. 1900163, doi: 10.1002/pssr.201900163.

[92] J. Carolus et al., "Why and how to adapt PID testing for bifacial PV modules?," *Prog. Photovolt.*, vol. 28, no. 10, pp. 1045–1053, 2020, doi: 10.1002/pip.3311.

[93] B. M. Cote, I. M. Slauch, T. J. Silverman, M. G. Deceglie, and V. E. Ferry, "Insulation or irradiance: Exploring why bifacial photovoltaics run hot," in *Proc. IEEE 48th Photovolt. Spec. Conf.*, 2021, pp. 1228–1232, doi: 10.1109/PVSC43889.2021.9518868.

[94] M. W. P. E. Lamers et al., "Temperature effects of bifacial modules: Hotter or cooler?," *Sol. Energy Mater. Sol. Cells*, vol. 185, pp. 192–197, Oct. 2018, doi: 10.1016/j.solmat.2018.05.033.

[95] O. Dupré, R. Vaillon, and M. A. Green, *Thermal Behavior of Photovoltaic Devices*. Berlin, Germany: Springer-Verlag, 2017, doi: 10.1007/978-3-319-49457-9.

[96] A. Sinha et al., "Glass/glass photovoltaic module reliability and degradation: A review," *J. Phys. D, Appl. Phys.*, vol. 54, no. 41, 2021, Art. no. 413002, doi: 10.1088/1361-6463/ac1462.

[97] F. Rahman et al., "Lamination process induced residual stress in glass-glass vs. glass-backsheet modules," presented at the IEEE Photovolt. Spec. Conf., Philadelphia, PA, USA, 2022.

[98] I. M. Slauch et al., "Manufacturing induced bending stresses: Glass-glass vs. glass-backsheet," in *Proc. IEEE 48th Photovolt. Spec. Conf.*, 2021, pp. 1943–1948, doi: 10.1109/PVSC43889.2021.9518938.

[99] N. Sheth et al., "Effects of tempering and heat strengthening on hardness, indentation fracture resistance, and wear of soda lime float glass," *Int. J. Appl. Glass Sci.*, vol. 10, no. 4, pp. 431–440, 2019, doi: 10.1111/ijag.13507.

[100] Vitro Architectural Glass, "Why annealed, heat strengthened and tempered glass all deflect the same amount," 2001. [Online]. Available: https://www.vitroglazings.com/media/xnsnzgog/vitro-td-113.pdf

[101] M. Kambe et al., "Chemically strengthened cover glass for preventing potential induced degradation of crystalline silicon solar cells," in *Proc. IEEE 39th Photovolt. Spec. Conf.*, 2013, pp. 3500–3503, doi: 10.1109/PVSC.2013.6744441.

[102] "Reducing the threat of hail damage to solar plants," Nextracker, 2021. Accessed: Aug. 12, 2022. [Online]. Available: https://www.nextracker.com/2021/03/reducing-the-threat-of-hail-damage-to-utility-scale-solar-plants/

[103] W. Gambogi et al., "Transparent backsheets for bifacial photovoltaic modules," in *Proc. IEEE 47th Photovolt. Spec. Conf.*, 2020, pp. 1651–1657, doi: 10.1109/PVSC45281.2020.9300924.

[104] S. Smith et al., "Transparent backsheets for bifacial photovoltaic (PV) modules: Material characterization and accelerated laboratory testing," *Prog. Photovolt., Res. Appl.*, vol. 30, no. 8, pp. 959–969, 2022, doi: 10.1002/pip.3494.

[105] C. Hirschl et al., "Determining the degree of crosslinking of ethylene vinyl acetate photovoltaic module encapsulants—A comparative study," *Sol. Energy Mater. Sol. Cells*, vol. 116, pp. 203–218, Sep. 2013, doi: 10.1016/j.solmat.2013.04.022.

[106] G. Oreski, A. Mihaljevic, Y. Voronko, and G. C. Eder, "Acetic acid permeation through photovoltaic backsheets: Influence of the composition on the permeation rate," *Polym. Testing*, vol. 60, pp. 374–380, 2017, doi: 10.1016/j.polymertesting.2017.04.025.

[107] G. Oreski et al., "Properties and degradation behaviour of polyolefin encapsulants for photovoltaic modules," *Prog. Photovolt.*, vol. 28, pp. 1277–1288, 2020, doi: 10.1002/pip.3323.

[108] B.-Å. Sultan and E. Sörvik, "Thermal degradation of EVA and EBA—A comparison. I. Volatile decomposition products," *J. Appl. Polym. Sci.*, vol. 43, no. 9, pp. 1737–1745, Nov. 1991, doi: 10.1002/app.1991.070430917.

[109] P. Klemchuk, M. Ezrin, G. Lavigne, W. Halley, and J. Galid, "Investigation of the degradation and stabilization of EVA-based encapsulant in field-aged solar energy modules," *Polym. Degradation Stability*, vol. 55, no. 3, pp. 347–365, 1997, doi: 10.1016/S0141-3910(96)00162-0.

[110] M. D. Kempe et al., "Acetic acid production and glass transition concerns with ethylene-vinyl acetate used in photovoltaic devices," *Sol. Energy Mater. Sol. Cells*, vol. 91, no. 4, pp. 315–329, 2007.

[111] U. Weber et al., "Acetic acid production, migration and corrosion effects in ethylene-vinyl-acetate-(EVA-) based PV modules," in *Proc. 27th Eur. Photovolt. Sol. Energy Conf. Exhib.*, 2012, pp. 2992–2995, doi: 10.4229/27thEUPVSEC2012-4CO.9.4.

[112] B. M. Habersberger, P. Hacke, and L. S. Madenjian, "Evaluation of the PID-s susceptibility of modules encapsulated in materials of varying resistivity," in *Proc. IEEE 7th World Conf. Photovolt. Energy Convers. (Joint Conf. 45th IEEE PVSC, 28th PVSEC, 34th EU PVSEC)*, 2018, pp. 3807–3809, doi: 10.1109/PVSC.2018.8548117.

[113] G. Oreski, B. Ottersböck, and A. Omazic, "Degradation processes and mechanisms of encapsulants," in *Durability and Reliability of Polymers and Other Materials in Photovoltaic Modules*. Norwich, NY, USA: William Andrew, 2019, pp. 135–152.

[114] G. Stollwerck, W. Schoeppel, A. Graichen, and C. Jaeger, "Polyolefin backsheet and new encapsulant suppress cell degradation in the module," in *Proc. 28th Eur. Photovolt. Sol. Energy Conf. Exhib.*, 2013, pp. 3318–3320, doi: 10.4229/28THEUPVSEC2013-4AV.5.44.

[115] J. Berghold, S. Koch, B. Frohmann, P. Hacke, and P. Grunow, "Properties of encapsulation materials and their relevance for recent field failures (IEEE 40th photovoltaic specialist conference)," presented at the IEEE 40th Photovolt. Spec. Conf., 2014, pp. 1987–1992.

[116] S. Pingel et al., "Potential induced degradation of solar cells and panels," in *Proc. IEEE 35th Photovolt. Spec. Conf.*, 2010, pp. 002817–002822, doi: 10.1109/PVSC.2010.5616823.

[117] M. C. López-Escalante et al., "Polyolefin as PID-resistant encapsulant material in PV modules," *Sol. Energy Mater.*, vol. 144, pp. 691–699, 2016, doi: 10.1016/j.solmat.2015.10.009.

[118] L. Spinella et al., "Chemical and mechanical interfacial degradation in bifacial glass/glass and glass/transparent backsheet photovoltaic modules," *Prog. Photovolt., Res. Appl.*, vol. 30, no. 12, pp. 1423–1432, Dec. 2022, doi: 10.1002/pip.3602.

[119] D. B. Sulas-Kern et al., "Electrochemical degradation modes in bifacial silicon photovoltaic modules," *Prog. Photovolt.*, vol. 30, no. 8, pp. 948–958, 2022, doi: 10.1002/pip.3530.

[120] S. K. Chunduri and M. Schmela, *Bifacial Solar Technology 2021—Part 1: Cells & Modules*. Dusseldorf, Germany: TaiyangNews, 2021.

[121] C. Ballif, F.-J. Haug, M. Boccard, P. J. Verlinden, and G. Hahn, "Status and perspectives of crystalline silicon photovoltaics in research and industry," *Nature Rev. Mater.*, vol. 7, no. 8, pp. 597–616, Aug. 2022, doi: 10.1038/s41578-022-00423-2.

[122] B. J. Hallam et al., "Development of advanced hydrogenation processes for silicon solar cells via an improved understanding of the behaviour of hydrogen in silicon," *Prog. Photovolt.*, vol. 28, no. 12, pp. 1217–1238, 2020, doi: 10.1002/pip.3240.

[123] S. Wilking, C. Beckh, S. Ebert, A. Herguth, and G. Hahn, "Influence of bound hydrogen states on BO-regeneration kinetics and consequences for high-speed regeneration processes," *Sol. Energy Mater. Sol. Cells*, vol. 131, pp. 2–8, Jan. 2014, doi: 10.1016/j.solmat.2014.06.027.

[124] N. E. Grant et al., "Lifetime instabilities in gallium doped monocrystalline PERC silicon solar cells," *Sol. Energy Mater. Sol. Cells*, vol. 206, 2020, Art. no. 110299, doi: 10.1016/j.solmat.2019.110299.

[125] N. E. Grant et al., "Gallium-doped silicon for high-efficiency commercial passivated emitter and rear solar cells," *Regional Res. Lab. Sol.*, vol. 5, no. 4, 2021, Art. no. 2000754, doi: 10.1002/solr.202000754.

[126] H. Steinkemper, M. Hermle, and S. W. Glunz, "Comprehensive simulation study of industrially relevant silicon solar cell architectures for an optimal material parameter choice: Study on silicon solar cell architectures," *Prog. Photovolt., Res. Appl.*, vol. 24, no. 10, pp. 1319–1331, Oct. 2016, doi: 10.1002/pip.2790.

[127] A. Augusto, J. Karas, P. Balaji, S. G. Bowden, and R. R. King, "Exploring the practical efficiency limit of silicon solar cells using thin solar-grade substrates," *J. Mater. Chem. A*, vol. 8, no. 32, pp. 16599–16608, 2020, doi: 10.1039/D0TA04575F.

[128] A. Richter, M. Hermle, and S. W. Glunz, "Reassessment of the limiting efficiency for crystalline silicon solar cells," *IEEE J. Photovolt.*, vol. 3, no. 4, pp. 1184–1191, Oct. 2013, doi: 10.1109/JPHOTOV.2013.2270351.

[129] K. Yoshikawa et al., "Silicon heterojunction solar cell with interdigitated back contacts for a photoconversion efficiency over 26%," *Nature Energy*, vol. 2, no. 5, May 2017, Art. no. 17032, doi: 10.1038/nenergy.2017.32.

[130] D. Lachenal et al., "Optimization of tunnel-junction IBC solar cells based on a series resistance model," *Sol. Energy Mater. Sol. Cells*, vol. 200, Sep. 2019, Art. no. 110036, doi: 10.1016/j.solmat.2019.110036.

[131] D. Chen et al., "Progress in the understanding of light- and elevated temperature-induced degradation in silicon solar cells: A review," *Prog. Photovolt., Res. Appl.*, vol. 29, no. 11, pp. 1180–1201, Nov. 2021, doi: 10.1002/pip.3362.

[132] K. Hara, S. Jonai, and A. Masuda, "Potential-induced degradation in photovoltaic modules based on n-type single crystalline Si solar cells," *Sol. Energy Mater. Sol. Cells*, vol. 140, pp. 361–365, 2015, doi: 10.1016/j.solmat.2015.04.037.

[133] S. Yamaguchi, B. B. Van Aken, A. Masuda, and K. Ohdaira, "Potential-induced degradation in high-efficiency n-type crystalline-silicon photovoltaic modules: A literature review," *Sol. Regional Res. Lab.*, vol. 5, no. 12, Dec. 2021, Art. no. 2100708, doi: 10.1002/solr.202100708.

[134] S. Yamaguchi, C. Yamamoto, K. Ohdaira, and A. Masuda, "Comprehensive study of potential-induced degradation in silicon heterojunction photovoltaic cell modules," *Prog. Photovolt., Res. Appl.*, vol. 26, no. 9, pp. 697–708, Sep. 2018, doi: 10.1002/pip.3006.

[135] S. Theingi et al., "Accelerated reliability tests of n+ and p+ poly-Si passivated contacts," *Sol. Energy Mater. Sol. Cells*, vol. 236, Mar. 2022, Art. no. 111469, doi: 10.1016/j.solmat.2021.111469.

[136] A. Sinha et al., "Assessing UV-induced degradation in bifacial modules of different cell technologies," in *Proc. IEEE 48th Photovolt. Spec. Conf.*, 2021, pp. 0767–0770, doi: 10.1109/PVSC43889.2021.9518728.

[137] J. Cattin et al., "Influence of light soaking on silicon heterojunction solar cells with various architectures," *IEEE J. Photovolt.*, vol. 11, no. 3, pp. 575–583, May 2021, doi: 10.1109/JPHOTOV.2021.3065537.

[138] D. Kang et al., "Long-term stability study of the passivation quality of polysilicon-based passivation layers for silicon solar cells," *Sol. Energy Mater. Sol. Cells*, vol. 215, Sep. 2020, Art. no. 110691, doi: 10.1016/j.solmat.2020.110691.

[139] W. Liu et al., "Damp-heat-stable, high-efficiency, industrial-size silicon heterojunction solar cells," *Joule*, vol. 4, no. 4, pp. 913–927, Apr. 2020, doi: 10.1016/j.joule.2020.03.003.

[140] T. Ishii and A. Masuda, "Annual degradation rates of recent crystalline silicon photovoltaic modules: Annual degradation rates of recent c-Si PV modules," *Prog. Photovolt., Res. Appl.*, vol. 25, no. 12, pp. 953–967, Dec. 2017, doi: 10.1002/pip.2903.

[141] Y. Zhang, M. Kim, L. Wang, P. Verlinden, and B. Hallam, "Design considerations for multi-terawatt scale manufacturing of existing and future photovoltaic technologies: Challenges and opportunities related to silver, indium and bismuth consumption," *Energy Environ. Sci.*, vol. 14, no. 11, pp. 5587–5610, 2021, doi: 10.1039/D1EE01814K.

[142] B. Grübel et al., "Progress of plated metallization for industrial bifacial TOPCon silicon solar cells," *Prog. Photovolt.*, vol. 30, no. 6, pp. 615–621, 2021, doi: 10.1002/pip.3528.

[143] J. Yu et al., "Copper metallization of electrodes for silicon heterojunction solar cells: Process, reliability and challenges," *Sol. Energy Mater. Sol. Cells*, vol. 224, 2021, Art. no. 110993, doi: 10.1016/j.solmat.2021.110993.

[144] N. Frasson and M. Galiazzo, "Evaluation of different approaches for HJT cells metallization based on low temperature copper paste," *Amer. Inst. Phys. Conf. Proc.*, vol. 2709, no. 1, 2022, Art. no. 020004, doi: 10.1063/5.0126222.

[145] N. Chen et al., "Thermal stable high-efficiency copper screen printed back contact solar cells," *Regional Res. Lab. Sol.*, vol. 7, no. 2, 2023, Art. no. 2200874, doi: 10.1002/solr.202200874.

[146] A. Lennon, J. Colwell, and K. P. Rodbell, "Challenges facing copper-plated metallisation for silicon photovoltaics," *Prog. Photovolt.*, vol. 27, pp. 67–97, 2018, doi: 10.1002/pip.3062.

[147] D. Adachi, T. Terashita, T. Uto, J. L. Hernández, and K. Yamamoto, "Effects of SiOx barrier layer prepared by plasma-enhanced chemical vapor deposition on improvement of long-term reliability and production cost for Cu-plated amorphous Si/crystalline Si heterojunction solar cells," *Sol. Energy Mater. Sol. Cells*, vol. 163, pp. 204–209, Apr. 2017, doi: 10.1016/j.solmat.2016.12.029.

[148] S. Kluska et al., "Plated TOPCon solar cells and modules with reliable fracture stress and soldered module interconnection," *Eur. Phys. J. Photovolt.*, vol. 12, p. 10, 2021, doi: 10.1051/epjpv/2021010.

Jarett Zuboy received the B.S. degree in geology from Colorado State University, Fort Collins, CO, USA, and the M.A. degree in history from the University of Colorado, Denver, CO, USA.

He is a Markets and Policy Analyst with the Strategic Energy Analysis Center, National Renewable Energy Laboratory, Golden, CO, USA. He has served as an Analyst and Writer on major solar energy reports for the U.S. Department of Energy, including the Solar Futures Study and SunShot Vision Study. His work focuses on technoeconomic analysis, supply chain issues, markets, and policy related to PV.

Martin Springer received the B.S., M.S., and Ph.D. degrees in mechanical engineering from the Vienna University of Technology, Vienna, Austria, in 2013, 2014, and 2017, respectively, and the MBA degree from the University of Colorado, Colorado Springs, CO, USA, in 2020.

He is a Researcher with the National Renewable Energy Laboratory, Golden, CO, USA. His current research interests focus on durability and reliability assessment of emerging PV cell interconnect technologies, cell and glass fracture in large-format PV modules, and performance degradation analysis of PV systems.

Elizabeth C. Palmiotti, originally from New York, received the B.S. degree in metallurgical and materials engineering in 2017 and the M.S. and Ph.D. degrees in materials science in 2021, all from the Colorado School of Mines, Golden, CO, USA.

She is currently a Postdoctoral Researcher with the National Renewable Energy Laboratory, Golden, CO, USA. Previously, she was a Postdoctoral Researcher with Sandia National Laboratories in Albuquerque, NM, USA. During her graduate studies, she was an IIE-GIRE Fellow and conducted her fellowship work with the Institut des Matériaux de Nantes, Université de Nantes, Nantes, France. She was an intern with the National Renewable Energy Laboratory during her undergraduate studies. Her research interests include thin-film PV, vapor deposition techniques, PV module packaging materials, and PV module reliability.

Joseph Karas received the B.S. degree in polymer science and engineering from Case Western Reserve University, Cleveland, OH, USA, in 2012 and the Ph.D. degree in materials science and engineering from Arizona State University, Tempe, AZ, USA, in 2020.

He is currently a Postdoctoral Researcher with the National Renewable Energy Laboratory's PV Reliability and System Performance Group, Golden, CO, USA, where he studies solar cell and module reliability.

Brittany L. Smith, photograph and biography not available at the time of publication.

Michael Woodhouse received the B.A. degree in secondary education (physics and chemistry) from the University of Wyoming, Laramie, WY, USA, and the Ph.D. degree in physical chemistry and materials science from Colorado State University, Fort Collins, CO, USA.

He is a Senior Analyst and Project Lead with the National Renewable Energy Laboratory (NREL), Golden, CO, USA. He currently leads a multiyear project focused on the design and development of NREL's cloud-based software platform for bottom-up component manufacturing and total system capital costs modeling (https://dcam.openei.org). As part of NREL's solar and storage technoeconomic analysis team, he has internationally recognized expertise in PV and storage system performance and levelized cost of electricity modeling, and he has worked on numerous projects for the U.S. Department of Energy's Solar Energy Technologies Office related to solar technology advancements and trade, supply chain, and policy issues. He also serves as an Associate Editor for energy economics and policy for the *Journal of Renewable and Sustainable Energy* and on the Steering Committee for the International Technology Roadmap for Photovoltaic.

Teresa M. Barnes received the B.S. degree in chemical engineering from the University of Maryland, College Park, MD, USA, and the Ph.D. degree in chemical engineering from the Colorado School of Mines, Golden, CO, USA.

She manages the Materials Reliability and Durability Group with the National Renewable Energy Laboratory (NREL), Golden, CO, USA. She is also the Principal Investigator and Director of the Dura-MAT Consortium for module materials research and a Distinguished Member of the Research Staff. Her group focuses on PV module and system reliability, including accelerated test development, materials and interface modeling, degradation mechanisms, field failure modes, sustainability, and materials science. The group she leads has worked with stakeholders throughout the PV value chain on the development of industry standards for reliability testing and energy yield. They conduct application-driven research on adhesion, cell and module degradation, mechanical damage, material weathering, and other topics. She has worked in PV at NREL for 20 years on thin-film PV, flexible devices, and transparent contacts and started focusing on reliability in 2016.